Atomic Data and Nuclear Data Tables 103–104 (2015) 4–49

Contents lists available at ScienceDirect

Atomic Data and Nuclear Data Tables

journal homepage: www.elsevier.com/locate/adt

Structure factors for tunneling ionization rates of diatomic molecules

Ryoichi Saito [a], Oleg I. Tolstikhin [b], Lars Bojer Madsen [c], Toru Morishita [a,*]

[a] Department of Engineering Science, The University of Electro-Communications, 1-5-1 Chofu-ga-oka, Chofu-shi, Tokyo 182-8585, Japan

[b] Moscow Institute of Physics and Technology, Dolgoprudny 141700, Russia

[c] Department of Physics and Astronomy, Aarhus University, 8000 Aarhus C, Denmark

ARTICLE INFO

Article history:
Received 23 April 2014
Received in revised form
29 January 2015
Accepted 7 February 2015
Available online 4 March 2015

keywords:
Tunneling ionization
Weak-field asymptotic theory
Structure factors
Diatomic molecules
Hartree–Fock oribitals

ABSTRACT

Within the leading-order, single-active-electron, and frozen-nuclei approximation of the weak-field asymptotic theory, the rate of tunneling ionization of a molecule in an external static uniform electric field is determined by the structure factor for the highest occupied molecular orbital. We present the results of systematic calculations of structure factors for 40 homonuclear and heteronuclear diatomic molecules by the Hartree–Fock method using a numerical grid-based approach implemented in the program X2DHF.

* Corresponding author.
E-mail address: toru@pc.uec.ac.jp (T. Morishita).

http://dx.doi.org/10.1016/j.adt.2015.02.001
0092-640X/

Contents

1. Introduction

The rate of tunneling ionization of atoms and molecules in an external static uniform electric field is an important property required for many applications in atomic, molecular, and optical physics. The current interest to this property is dictated by its applications in strong-field physics and attoscience [1], where tunneling ionization is the initial key process that triggers subsequent dynamics [2,3]. In the adiabatic regime of main interest for such applications, that is, at sufficiently low frequency and high intensity, tunneling ionization in an oscillating laser field proceeds as if the field were static and equal to its instantaneous value [4,5].

Recently, we have developed the weak-field asymptotic theory (WFAT) of tunneling ionization [6]. This theory generalizes the earlier treatments of tunneling ionization from spherically symmetric atomic potentials [7–10] to molecular potentials without any symmetry. In the WFAT, the ionization rate is sought as an asymptotic expansion in the field F. Such an approach is justified for sufficiently weak fields satisfying $F \ll F_c$, where F_c is a field at which over-the-barrier ionization becomes accessible. Since for neutral atoms and molecules in the ground state $F_c \sim 0.1$ a.u., which corresponds to a laser intensity $I \sim 3.5 \times 10^{14}$ W/cm^2, the WFAT applies to all truly static fields available in laboratories as well as to the majority of intense low-frequency laser pulses used in current experiments.

The leading-order term in the asymptotic expansion for the ionization rate of an arbitrary molecule treated in the single-active-electron (SAE) and frozen-nuclei (FN) approximations was obtained in Ref. [6]. Under these approximations, tunneling ionization occurs from the highest occupied molecular orbital (HOMO) taken at the equilibrium internuclear configuration. The ionization rate of a molecule depends on the field and orientation of the molecule with respect to the field; these two dependences are of main interest for applications. In the formula for the rate obtained in Ref. [6] these dependences factorize. The field-dependent factor is a simple analytic function of F and the ionization potential of the HOMO. The orientation-dependent factor, given by the *structure factor* squared, depends on the dipole moment of the HOMO and a coefficient appearing in its asymptotic tail. The structure factor is as fundamental a property of a molecule as, e.g., its static dipole polarizability; in fact, the two characteristics play similar roles in evaluating the tunneling ionization rate and second-order Stark shift, respectively. Since the field factor is known analytically, the calculation of the ionization rate within the WFAT reduces to calculating the structure factor. The techniques for calculating molecular structure factors based on the different quantum chemistry codes were developed in Refs. [11–13]. In this work, we present the results of systematic calculations of structure factors for 40 homonuclear and heteronuclear diatomic molecules by the Hartree–Fock (HF) method using the program X2DHF [14]. With these results at hands, the ionization rates of the molecules can be readily evaluated.

Let us emphasize that the structure factors presented below enable one to obtain only the leading-order term in the asymptotic expansion of the ionization rate in F evaluated in the SAE and FN approximations. This basic approximation of the WFAT [6] is now a well established theory, and this paper presents an extensive set of results within this theory. At the same time, it should be noted that a number of generalizations of the WFAT is already available. Thus the first-order correction terms in the asymptotic expansion of the rate in F were derived in Refs. [15,16]; the incorporation of the effects of nuclear motion within the WFAT was discussed in Refs. [17,18]; a generalization of the WFAT to many-electron systems was developed in Refs. [19,20]. The evaluation of the rate within these generalizations requires much more involved calculations beyond the basic WFAT employed in this work. Atomic units are used throughout the paper.

2. Theory

In this section, we summarize formulas needed to implement the basic WFAT [6] for linear molecules, which includes diatomic molecules as a particular case. We introduce laboratory and molecular coordinate frames. Let $\mathbf{r} = (x, y, z)$ and $\mathbf{r}' = (x', y', z')$ denote the Cartesian coordinates of the active electron in these frames, respectively, and $\hat{R}$ denote an Euler rotation [21] from the laboratory to the molecular frame, $\mathbf{r}' = \hat{R}\mathbf{r}$. By our convention, the z axis is directed along the electric field, thus the field is $\mathbf{F} = F\mathbf{e}_z, F > 0$; the z' axis coincides with the internuclear axis and lies in the xz plane; the y and y' axes coincide. Then the different orientations of the molecule with respect to the field are described by a single angle β, $0 \leqslant \beta \leqslant \pi$, defining the rotation $\hat{R}$ from z to z' about the $y = y'$ axis. Explicitly, the relations between the coordinates read

$$x' = x\cos\beta - y\sin\beta, \tag{1a}$$

$$y' = y, \tag{1b}$$

$$z' = x\sin\beta + z\cos\beta. \tag{1c}$$

Let $E < 0$ and $\psi(\mathbf{r}')$ be the energy and wave function of the unperturbed field-free HOMO in the molecular frame. The structure of $\psi(\mathbf{r}')$ assumed must be explained. The unperturbed orbitals $\psi_M(\mathbf{r}')$ of linear molecules can be generally characterized by the projection $M = 0, \pm1, \pm2, \ldots$ of the electronic angular momentum onto the internuclear axis. We have $\psi_M(\mathbf{r}') \propto e^{iM\varphi'}$, where φ' is the azimuthal angle in the molecular frame. The orbital energy does not depend on the sign of M, therefore states with $M \neq 0$ are doubly degenerate. This degeneracy is removed by an arbitrarily weak field, provided that the molecule is not aligned along the field. The correct zeroth-order orbitals (in the sense of perturbation theory for degenerate states [7]) in our geometry are given by

$$\psi^{(+)}_{|M|}(\mathbf{r}') = \frac{1}{\sqrt{2}}\left[\psi_M(\mathbf{r}') + \psi_{-M}(\mathbf{r}')\right], \tag{2a}$$

$$\psi^{(-)}_{|M|}(\mathbf{r}') = \frac{1}{i\sqrt{2}}\left[\psi_M(\mathbf{r}') - \psi_{-M}(\mathbf{r}')\right]. \tag{2b}$$

The functions $\psi^{(\lambda)}_{|M|}(\mathbf{r}')$ with $\lambda = +$ and $-$ are even and odd under the reflection $y' \to -y'$, respectively. They both are chosen to be real. The orbital $\psi(\mathbf{r}')$ has the form of $\psi^{(\lambda)}_{|M|}(\mathbf{r}')$, and hence is real and characterized by the absolute value of the projection $|M|$ and parity λ. We suppress these indexes in the notation for brevity. In the following, we assume that $M \geqslant 0$. In addition, it is assumed that $\psi(\mathbf{r}')$ is normalized to 1. Let us introduce the dipole moment of the HOMO in the molecular frame,

$$\boldsymbol{\mu}' = -\int \mathbf{r}'\psi^2(\mathbf{r}')\,d\mathbf{r}' = \mu\mathbf{e}_{z'}. \tag{3}$$

The dipole moment in the laboratory frame is $\boldsymbol{\mu} = \hat{R}^{-1}\boldsymbol{\mu}'$.

Within the WFAT [6], the problem of tunneling ionization is treated in parabolic coordinates defined by [7]

$$\xi = r + z, \quad 0 \leqslant \xi < \infty, \tag{4a}$$

$$\eta = r - z, \quad 0 \leqslant \eta < \infty, \tag{4b}$$

$$\varphi = \arctan\frac{y}{x}, \quad 0 \leqslant \varphi < 2\pi. \tag{4c}$$

The total ionization rate Γ in the weak-field limit is given by a sum of partial rates for ionization into parabolic channels labeled by (n_ξ, m), where $n_\xi = 0, 1, 2, \ldots$ and $m = 0, \pm1, \pm2, \ldots$ are parabolic quantum numbers of the ionized electron. The different channels contribute to the different orders in the asymptotic expansion of Γ for $F \to 0$, and the dominant contribution comes from the *dominant* ionization channels. The dominant channels are $(0, \pm\bar{m})$, where the value of $\bar{m} \geqslant 0$ depends on the orientation of the molecule and symmetry of the HOMO. If the molecule is aligned along the field, then $\bar{m} = M$; otherwise, $\bar{m} = 0$ for even $(\lambda = +)$ states with $M \geqslant 0$ and $\bar{m} = 1$ for odd $(\lambda = -)$ states with $M \geqslant 1$. Each partial rate in turn is given by an asymptotic expansion in F. Thus in the leading-order approximation Γ is given by a sum of the leading-order terms in the expansions of partial rates for the dominant channels. For a given $\bar{m}$, the resulting formula for the ionization rate reads

$$\Gamma = (2 - \delta_{\bar{m}0})|G_{0\bar{m}}(\beta)|^2 W_{0\bar{m}}(F). \tag{5}$$

Although in the leading-order approximation Γ is determined by the contributions from the dominant channels with $n_\xi = 0$, as is indicated by the subscripts of the factors in Eq. (5), the first-order correction terms [15,16] involve channels with $n_\xi > 0$, so it is worthwhile to define the factors for an arbitrary channel (n_ξ, m). The *structure factor*,

$$G_{n_\xi m}(\beta) = \lim_{\eta\to\infty} G_{n_\xi m}(\beta;\eta), \tag{6}$$

is given by the asymptotic value of the *structure function*,

$$G_{n_\xi m}(\beta;\eta) = e^{-\varkappa\mu_z}\eta^{1+|m|/2-Z/\varkappa}e^{\varkappa\eta/2} \times \int_0^\infty\int_0^{2\pi} \phi_{n_\xi m}(\xi)\frac{e^{-im\varphi}}{\sqrt{2\pi}}\psi(\hat{R}\mathbf{r})\,d\xi\,d\varphi, \tag{7}$$

and the *field factor* is

$$W_{n_\xi m}(F) = \frac{\varkappa}{2}\left(\frac{4\varkappa^2}{F}\right)^{2Z/\varkappa-2n_\xi-|m|-1}\exp\left(-\frac{2\varkappa^3}{3F}\right). \tag{8}$$

Here $\varkappa = \sqrt{2|E|}$, Z is the charge of the molecular ion after tunneling ionization ($Z = 1$ for neutral molecules), $\mu_z = \mu\cos\beta$ is the z-component of $\boldsymbol{\mu}$, and $\phi_{n_\xi m}(\xi)$ is a parabolic channel function,

$$\phi_{n_\xi m}(\xi) = \varkappa^{1/2}(\varkappa\xi)^{|m|/2}e^{-\varkappa\xi/2}\sqrt{\frac{n_\xi!}{(n_\xi+|m|)!}}L^{(|m|)}_{n_\xi}(\varkappa\xi), \tag{9}$$

where $L^{(\alpha)}_n(x)$ are the generalized Laguerre polynomials [22]. The structure factor (6) depends on the orientation angle β through μ_z and $\hat{R}$ in Eq. (7). Note that it does not depend on the field F and, on the other hand, the field factor (8) does not depend on β, thus these dependences in Eq. (5) factorize. While $W_{n_\xi m}(F)$ is known explicitly, $G_{n_\xi m}(\beta)$ is a nontrivial characteristic determined by the asymptotic tail of the HOMO. To implement Eq. (5), one needs to extract $G_{0\bar{m}}(\beta)$ from the HOMO — such calculations are the subject of this work. From Eqs. (6) and (7) one obtains

$$G_{00}(\beta) = e^{-\varkappa\mu_z}\sqrt{\frac{2\pi}{\varkappa}}\,|2z|^{1-Z/\varkappa}e^{\varkappa|z|}\psi(\hat{R}\mathbf{r})\Big|_{x=y=0,\,z\to-\infty}, \tag{10}$$

which gives another representation for $G_{00}(\beta)$.

To compress the information needed for applications, the structure factor (6) as a function of the orientation angle β can be expanded in terms of an appropriate set of standard functions. It is convenient to use the expansion [11]

$$G_{n_\xi m}(\beta) = i^p\sum_{l=|M-m|}^{\infty} C^{(l)}_{n_\xi m}\Theta_{l|M-m|}(\cos\beta), \tag{11}$$

where $p = 0$ $(p = 1)$ for even (odd) states, $C^{(l)}_{n_\xi m}$ are the *structure coefficients*, and $\Theta_{lm}(x)$ are given in terms of the associated Legendre polynomials $P^m_l(x)$ [21],

$$\Theta_{lm}(x) = \sqrt{\frac{(2l+1)(l-m)!}{2(l+m)!}}\,P^m_l(x). \tag{12}$$

In Eq. (11) it is assumed that $m \geqslant 0$; with the present assumptions regarding $\psi(\mathbf{r}')$, the structure factors for negative m can be obtained from $G_{n_\xi,-m}(\beta) = G^*_{n_\xi m}(\beta)$. The factor i^p in Eq. (11) ensures that for all states and ionization channels the structure coefficients are real. The goal of the present calculations is to tabulate the coefficients $C^{(l)}_{0\bar{m}}$ for the molecules under consideration. Given these coefficients, the structure factor $G_{0\bar{m}}(\beta)$ and the ionization rate (5) can be readily calculated.

These formulas describe tunneling ionization from a given orbital. Let us discuss briefly how to obtain the total ionization rate of a molecule. Tunneling ionization from inner orbitals is suppressed by the exponential factor in Eq. (8), because of a larger ionization potential. That is why the total ionization rate of a molecule is determined by that of the HOMO. If the HOMO is not degenerate, as is the case for states with $M = 0$, the total ionization rate coincides with that of the HOMO multiplied by the number of electrons in the HOMO. For example, for $H_2(1\sigma_g^2)$ and $BeH(3\sigma)$ (only the HOMO in the electronic configuration is indicated) this number is 2 and 1, respectively. In the case of a degenerate HOMO with $M > 0$, tunneling ionization from the even state $(\bar{m} = 0)$ dominates over that from the odd state $(\bar{m} = 1)$, because of the additional power of F in Eq. (8) in the latter case. Then the total ionization rate of a molecule is given by that of the even HOMO, again multiplied by the number of electrons in the HOMO. For example, there are two electrons in the even HOMO in $C_2(1\pi_u^4)$. However, the structure factor for the dominant ionization channel with $\bar{m} = 0$ for the even HOMO vanishes at the parallel orientation, when the molecule is aligned along the field. In this case even and odd HOMOs produce equal contributions to the total ionization rate. Their contributions remain comparable at near-parallel orientations. To obtain the total ionization rate in this special case the first-order [15,16] and many-electron [19,20] theories must be employed, which is beyond the scope of the present paper. We just mention that this analysis requires to know the structure factor for the odd HOMO. Moreover, in cases where the degenerate HOMO is not completely occupied,

e.g. CH(1π), the molecule can be initially prepared in a state containing no electrons in the even HOMO, and then tunneling ionization from the odd HOMO becomes the dominant process. All this shows that for molecules with degenerate HOMO structure factors for both even and odd states are needed for applications.

To conclude this section, let us summarize the approximations under which Eq. (5) applies and where its validations are available. We first discuss the case of a static field. The main condition of applicability of the WFAT is

$$F \ll F_c \approx \frac{\varkappa^4}{8|2Z - \varkappa(\bar{m}+1)|}, \tag{13}$$

where F_c is the boundary of the over-the-barrier ionization regime. For one electron in a model potential, the assumption that the field is sufficiently weak is the only approximation. In this case, the validity of the WFAT was confirmed by comparison with the results of accurate calculations of tunneling ionization rates from atomic [15] and molecular [16,23,24] potentials by the Siegert-state method. In addition, the present calculations for diatomic molecules employ the SAE and FN approximations. To estimate an error incurred by the SAE approximation accurate fully-correlated *ab initio* results for tunneling ionization rates of many-electron systems are required. Such calculations were reported only for several atoms H^- [25], He [26–28], and Li [29] and one molecule H_2 at a single orientation $\beta = 0$ [30]. Comparison of their results with the results of the many-electron WFAT [19,20] shows that, at least for the few-electron systems considered, the SAE approximation in combination with the use of the HF orbitals works rather well, its effect on the value of the structure factors does not exceed a few percent. A more essential departure from the SAE approximation can be expected in systems with strong configuration interaction in the field-free initial state, which is the case, e.g., if the energy spacing between the HOMO and the next inner orbital is small. In Ref. [13] we have compared the WFAT results for a water molecule H_2O obtained in the SAE approximation implemented by means of the HF and density functional one-electron orbitals. While the latter approach has the advantage of enabling one to incorporate into the theory the exact ionization potential of the system, which may have an effect on the field factor (8), the structure factors (6) obtained by the two approaches are very close to each other. This justifies the use of the HF orbitals in the present calculations of the molecular structure factors. Finally, the error incurred by the FN approximation can be estimated by incorporating the effect of the internuclear motion into the WFAT within the Born–Oppenheimer approximation. Our calculations for H_2 [17] show that the effect strongly depends on the initial vibrational state and becomes more essential at weaker fields. However, recently it was realized that the Born–Oppenheimer approximation breaks down in the theory of tunneling ionization at sufficiently weak fields [18]. Thus the effect of the internuclear motion on the tunneling ionization rate of an electron requires further studies. In the present calculations we employ the FN approximation.

The application of the WFAT to tunneling ionization in laser fields with characteristic amplitude F and frequency ω is additionally restricted by the condition of applicability of the adiabatic approximation $\omega \ll F^2/\varkappa^4$ [5]. We mention that there exists a number of *ab initio* time-dependent calculations treating the interaction of diatomic molecules with near-infrared laser pulses (see, e.g., Refs. [31–36]). A qualitative comparison of the WFAT results with such calculations can be found in [11–13].

3. Computational procedure

In Ref. [11] we demonstrated how the above equations can be implemented within the HF method using the program X2DHF [14]. More recently, some additional computational techniques for linear [12] and nonlinear [13] molecules were developed and tested. With this experience, we have performed systematic calculations of the structure factors and structure coefficients for 40 diatomic molecules in the ground state. In this section we discuss some details of the calculations.

The orientation angle β will be measured in degrees. As seen from Eqs. (1), at $\beta = 0^\circ$ the molecule is aligned along the field. By our convention, the orientation of a heteronuclear molecule with respect to the field in this case is determined by its notation, namely, atoms A and B of a molecule AB are located at the negative and positive sides of the z-axis, respectively. The coordinate origin is chosen to be at the geometrical center between the nuclei. The value of the dipole moment μ, see Eq. (3), depends on the origin and hence is affected by this choice, but the structure factor (6) is invariant under a translation of the origin along the z-axis [6]. The internuclear distance R is set equal to its equilibrium value. When available, the experimental equilibrium distances from Ref. [37] are used; otherwise we used the value of R at the minimum of the Born–Oppenheimer potential calculated by the HF method. For all molecules considered, the HOMO $\psi(\mathbf{r}')$ is either a σ-state ($M = 0$) or a π-state ($M = 1$). The σ-states are even and for them $\bar{m} = 0$ at all β. As discussed above, we consider both even and odd π-states. They have a nodal plane which at $\beta = 0$ coincides with the yz and xz plane, respectively. It is convenient to identify these states by the nodal plane and denote the even and odd π-states by (yz) and (xz), respectively. We use this notation in the tables and figures to follow. For the (yz) states we generally have $\bar{m} = 0$, except for the parallel orientations with $\beta = 0^\circ$ and 180°, when $\bar{m} = 1$. We present the results for $\bar{m} = 0$; a change of the dominant ionization channel at the parallel orientations is related to vanishing of the structure factor $G_{00}(\beta)$ at $\beta = 0^\circ$ and 180°. For the (xz) states we have $\bar{m} = 1$ at all β.

For a given molecule, we first calculate the energy E, wave function $\psi(\mathbf{r}')$ and dipole moment μ of the HOMO. The symmetry of the HOMO defines the value of $\bar{m}$ as described above. Then we fix the orientation angle β and calculate the structure function $G_{0\bar{m}}(\beta;\eta)$ using Eq. (7). The structure factor $G_{0\bar{m}}(\beta)$ is obtained in the following way [12]. The $G_{0\bar{m}}(\beta;\eta)$ is considered as a function of the reciprocal variable $t = 1/\eta$. It is calculated at $N_{\rm pnt}$ equidistant points in the interval $1/\eta_{\max} \leqslant t \leqslant 1/\eta_{\min}$. The values obtained are fitted by a polynomial of degree $N_{\rm pln}$,

$$G_{0\bar{m}}(\beta;\eta) = \sum_{n=0}^{N_{\rm pln}} c_n(\beta) t^n. \tag{14}$$

For the majority of molecules, the function $G_{0\bar{m}}(\beta;\eta)$ calculated using a HOMO $\psi(\mathbf{r}')$ from X2DHF monotonically converges to a constant as η grows beyond $\eta \sim 10$. But in some cases this function demonstrates a nonmonotonic behavior at large η. In order to extract as accurate results as possible, depending on the behavior of $\psi(\mathbf{r}')$ in the asymptotic region one of the following three sets of the fitting parameters was used:

$$\text{A:}\quad \eta_{\min} = 10,\quad \eta_{\max} = 60,\quad N_{\rm pnt} = 80,\quad N_{\rm pln} = 12, \tag{15a}$$

$$\text{B:}\quad \eta_{\min} = 10,\quad \eta_{\max} = 70,\quad N_{\rm pnt} = 80,\quad N_{\rm pln} = 12, \tag{15b}$$

$$\text{C:}\quad \eta_{\min} = 5,\quad \eta_{\max} = 20,\quad N_{\rm pnt} = 80,\quad N_{\rm pln} = 25. \tag{15c}$$

The fitting procedure returns the coefficients $c_n(\beta)$ in Eq. (14). The structure factor is given by $G_{0\bar{m}}(\beta) = c_0(\beta)$. The calculations are repeated with the step of 1° in β. Then the structure coefficients $C^{(l)}_{0\bar{m}}$ are calculated.

4. Results

The results for the 40 diatomic molecules considered are presented in the tables and figures. As an example, let us discuss

briefly the H_2 molecule. Table 1 gives the configuration and term of the molecule and symmetry of the HOMO, the equilibrium internuclear distance, the energy and electronic dipole moment of the HOMO, and the set of fitting parameters defined in Eqs. (15). The following table with the structure coefficients $C_{00}^{(l)}$ in combination with Eq. (11) defines the structure factor $G_{00}(\beta)$. This factor squared as a function of β is displayed in Graph 1. The graph shows that the ionization rate (5) peaks when the molecule is aligned along the field and minimizes at the perpendicular orientation. Tables 2–40 and Graphs 2–40 provide similar information for the other molecules. For molecules with a π-state HOMO (see, e.g., Table 4 and Graph 4 for B_2), the results for both even (yz) and odd (xz) states are given.

We note that the structure factor for the dominant ionization channel $G_{0\bar{m}}(\beta)$ may turn to zero at some special values of β. This is always the case at $\beta = 0°$ and 180° for the even (yz) state in the case of a π-state HOMO (see, e.g., Graph 4 for B_2) and at $\beta = 90°$ for homonuclear molecules whose HOMO has a node in the $x'z'$ plane (see, e.g., Graph 3 for Be_2 and Graph 7 for O_2 as examples of σ- and π-state HOMOs with a node, respectively), but this may also happen at some intermediate orientation β for heteronuclear molecules (see, e.g., Graph 10 for BeH). At such special orientations the contribution to the ionization rate from the dominant ionization channel vanishes, which means that the next-to-the-dominant ionization channel with larger values of n_ξ and $|m|$ in Eq. (8) must be taken into account (for more details on this point see the analysis in Ref. [11]).

5. Conclusion

This work presents the first extensive compilation of structure coefficients for 40 diatomic molecules in the ground state calculated with the use of the HF orbitals. The structure coefficients determine the molecular structure factor, which in turn determines within the leading-order, SAE, and FN approximation of the WFAT [6] dependence of the tunneling ionization rate on the orientation of the molecule with respect to the external electric field. The extraction of the structure factor requires an accurate description of the asymptotic part of the HOMO, which is in general tedious to obtain by standard quantum chemistry basis-based approaches (see the discussion in Refs. [11,13]), but was achieved here for the diatomics using a numerical grid-based approach as implemented in the program X2DHF [14]. Within the HF method, the present tables and graphs give molecular structure factors needed to implement the WFAT to unprecedented precision.

Acknowledgments

This work was supported in part by Grants-in-Aid for Scientific Research (A), (B), and (C) from the Ministry of Education, Culture, Sports, Science and Technology, Japan. O. I. T. acknowledges the support from the Russian Foundation for Basic Research (Grant No. 14-02-92110) and the Ministry of Education and Science of Russia (State assignment No. 3.679.2014/K). L. B. M. acknowledges support from an ERC-StG (Project No. 277767-TDMET).

References

[1] F. Krausz, M. Ivanov, Rev. Modern Phys. 81 (2009) 163.
[2] P.B. Corkum, Phys. Rev. Lett. 71 (1993) 1994.
[3] T. Morishita, A.-T. Le, Z. Chen, C.D. Lin, Phys. Rev. Lett. 100 (2008) 013903.
[4] L.V. Keldysh, Zh. Eksp. Teor. Fiz. 47 (1964) 1945 [Sov. Phys. JETP 20 (1965) 1307].
[5] O.I. Tolstikhin, T. Morishita, Phys. Rev. A 86 (2012) 043417.
[6] O.I. Tolstikhin, T. Morishita, L.B. Madsen, Phys. Rev. A 84 (2011) 053423.
[7] L.D. Landau, E.M. Lifshitz, Quantum Mechanics (Non-relativistic Theory), Pergamon Press, Oxford, 1977.
[8] B.M. Smirnov, M.I. Chibisov, Zh. Eksp. Teor. Fiz. 49 (1965) 841 [Sov. Phys. JETP 22 (1966) 585].
[9] S.Yu. Slavyanov, Problemy Matematicheskoi Fiziki 4 (1970) 125. English translation in: Topics in Mathematical Physics, vol. 4, Consultants Bureau, New York–London, 1971.
[10] T. Yamabe, A. Tachibana, H.J. Silverstone, Phys. Rev. A 16 (1977) 877.
[11] L.B. Madsen, O.I. Tolstikhin, T. Morishita, Phys. Rev. A 85 (2012) 053404.
[12] L.B. Madsen, F. Jensen, O.I. Tolstikhin, T. Morishita, Phys. Rev. A 87 (2013) 013406.
[13] L.B. Madsen, F. Jensen, O.I. Tolstikhin, T. Morishita, Phys. Rev. A 89 (2014) 033412.
[14] J. Kobus, L. Laaksonen, D. Sundholm, Comput. Phys. Commun. 98 (1996) 346. http://www.leiflaaksonen.eu/num2d.html.
[15] V.H. Trinh, O.I. Tolstikhin, L.B. Madsen, T. Morishita, Phys. Rev. A 87 (2013) 043426.
[16] V.H. Trinh, V.N.T. Pham, O.I. Tolstikhin, T. Morishita, in preparation.
[17] O.I. Tolstikhin, H.J. Wörner, T. Morishita, Phys. Rev. A 87 (2013) 041401(R).
[18] O.I. Tolstikhin, L.B. Madsen, Phys. Rev. Lett. 111 (2013) 153003.
[19] O.I. Tolstikhin, L.B. Madsen, T. Morishita, Phys. Rev. A 89 (2014) 013421.
[20] I.Yu. Tolstikhina, T. Morishita, O.I. Tolstikhin, Phys. Rev. A 90 (2014) 053413.
[21] A.R. Edmonds, Angular Momentum in Quantum Mechanics, Princeton University Press, Princeton, 1957.
[22] M. Abramowitz, I.A. Stegun (Eds.), Handbook of Mathematical Functions, Dover Publications Inc., New York, 1972.
[23] L. Hamonou, T. Morishita, O.I. Tolstikhin, Phys. Rev. A 86 (2012) 013412.
[24] V.N.T. Pham, O.I. Tolstikhin, T. Morishita, Phys. Rev. A 89 (2014) 033426.
[25] S.I. Themelis, C.A. Nicolaides, Phys. Rev. A 49 (1994) 3089.
[26] A. Scrinzi, M. Geissler, T. Brabec, Phys. Rev. Lett. 83 (1999) 706.
[27] S.I. Themelis, T. Mercouris, C.A. Nicolaides, Phys. Rev. A 61 (1999) 024101.
[28] J.S. Parker, G.S.J. Armstrong, M. Boca, K.T. Taylor, J. Phys. B 42 (2009) 134011.
[29] S.I. Themelis, C.A. Nicolaides, J. Phys. B 33 (2000) 5561.
[30] A. Saenz, Phys. Rev. A 66 (2002) 063408.
[31] S.-K. Son, S.-I. Chu, Chem. Phys. 366 (2009) 91.
[32] E. Dehghanian, A.D. Bandrauk, G. Lagmago Kamta, Phys. Rev. A 81 (2010) 061403(R).
[33] Y.-J. Jin, X.-M. Tong, N. Toshima, Phys. Rev. A 83 (2011) 063409.
[34] X. Chu, M. McIntyre, Phys. Rev. A 83 (2011) 013409.
[35] E. Dehghanian, A.D. Bandrauk, G. Lagmago Kamta, J. Chem. Phys. 139 (2013) 084315.
[36] E.F. Penka, E. Couture-Bienvenue, A.D. Bandrauk, Phys. Rev. A 89 (2014) 023414.
[37] NIST Standard Reference Database 101, Computational Chemistry Comparison and Benchmark Database, 2013; http://cccbdb.nist.gov/.

Explanation of Tables

Tables 1–40.	**Structure coefficients**
Orbital	Electronic configuration and molecular term in the ground state; the HOMO from which tunneling ionization occurs is underlined.
R	Equilibrium internuclear distance from Ref. [37]; if not available in Ref. [37], the internuclear distance at the minimum of the HF Born–Oppenheimer potential is given, which is indicated by (HF).
E	Energy of the HOMO.
μ	Electronic dipole moment of the HOMO.
Fit	Set of fitting parameters as defined in Eqs. (15).
l	Summation index in Eq. (11).
$C_{0\bar{m}}^{(l)}$	Structure coefficients in Eq. (11), the value of $\bar{m}$ is apparent from the subscript.

The notation $a[b] = a \times 10^b$ is used throughout.

Explanation of Graphs

Graphs 1–40.	**Orientation dependence of the structure factor squared**
β	Orientation angle in degrees.
$G_{0\bar{m}}(\beta)$	Structure factor.

Table 1
Structure coefficients for H_2.

Orbital	R	E	μ	Fit
$1\sigma_g^2, X^1\Sigma_g^+$	1.4011	−0.5944789	0	A

l	$C_{00}^{(l)}$	l	$C_{00}^{(l)}$
0	2.465	6	1.795[−6]
2	1.069[−1]	8	9.233[−7]
4	1.012[−3]	10	−2.537[−6]

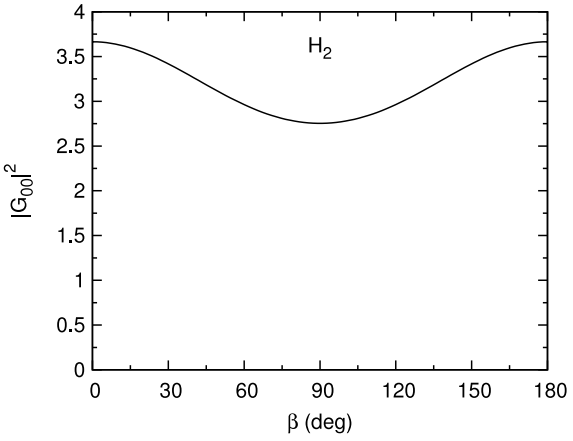

Graph 1. Orientation dependence of the structure factor squared for H_2.

Table 2
Structure coefficients for Li_2.

Orbital	R	E	μ	Fit
$1\sigma_g^2 1\sigma_u^2 2\sigma_g^2, X^1\Sigma_g^+$	5.0512	−0.1819483	0	B

l	$C_{00}^{(l)}$	l	$C_{00}^{(l)}$
0	5.688[−1]	6	1.886[−5]
2	6.815[−2]	8	1.606[−6]
4	1.804[−3]	10	2.002[−6]

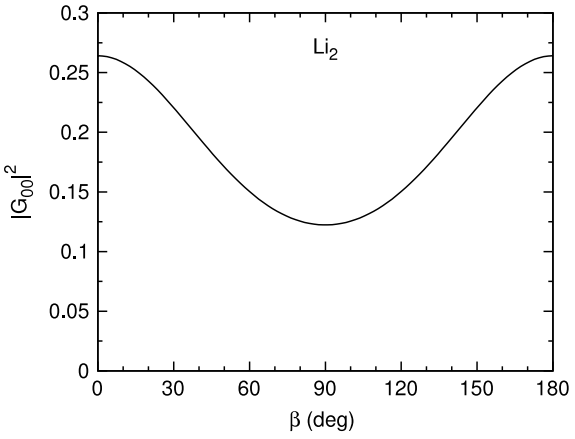

Graph 2. Orientation dependence of the structure factor squared for Li_2.

Table 3
Structure coefficients for Be_2.

Orbital	R	E	μ	Fit
$1\sigma_g^2 1\sigma_u^2 2\sigma_g^2 2\sigma_u^2, {}^1\Sigma_g^+$	4.6487	−0.2432928	0	B

l	$C_{00}^{(l)}$	l	$C_{00}^{(l)}$
1	1.268	7	4.640[−5]
3	1.138[−1]	9	2.244[−6]
5	3.240[−3]		

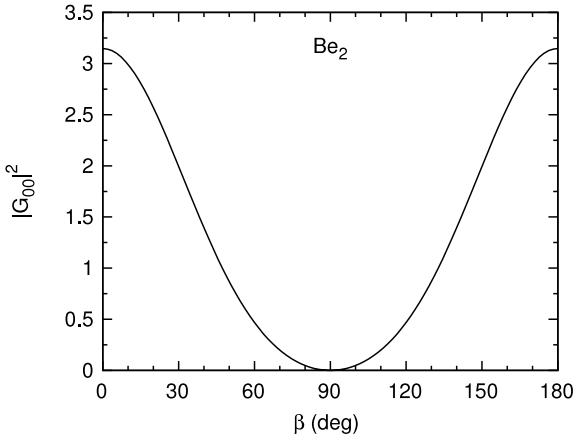

Graph 3. Orientation dependence of the structure factor squared for Be_2.

Table 4
Structure coefficients for B_2.

Orbital	R	E	μ	Fit
$1\sigma_g^2 1\sigma_u^2 2\sigma_g^2 2\sigma_u^2 1\pi_u^2, X^3\Sigma_g^-$	3.0047	−0.3594307	0	B

(yz) state				(xz) state			
l	$C_{00}^{(l)}$	l	$C_{00}^{(l)}$	l	$C_{01}^{(l)}$	l	$C_{01}^{(l)}$
1	2.049	7	3.754[−5]	0	2.870	6	7.667[−5]
3	1.706[−1]	9	4.874[−8]	2	3.221[−1]	8	3.486[−7]
5	3.782[−3]			4	7.526[−3]	10	−3.120[−8]

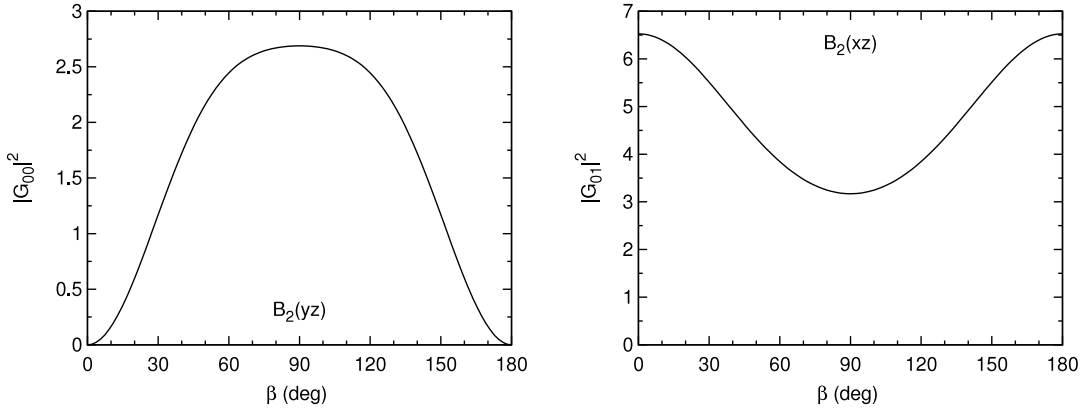

Graph 4. Orientation dependence of the structure factor squared for B_2.

Table 5
Structure coefficients for C_2.

Orbital	R	E	μ	Fit
$1\sigma_g^2 1\sigma_u^2 2\sigma_g^2 2\sigma_u^2 1\pi_u^4, X^1\Sigma_g^+$	2.3480	−0.4580192	0	B

(yz) state				(xz) state			
l	$C_{00}^{(l)}$	l	$C_{00}^{(l)}$	l	$C_{01}^{(l)}$	l	$C_{01}^{(l)}$
1	2.322	7	4.594[−5]	0	3.066	6	8.799[−5]
3	1.995[−1]	9	2.207[−7]	2	3.547[−1]	8	4.929[−7]
5	4.543[−3]			4	8.510[−3]	10	−4.623[−9]

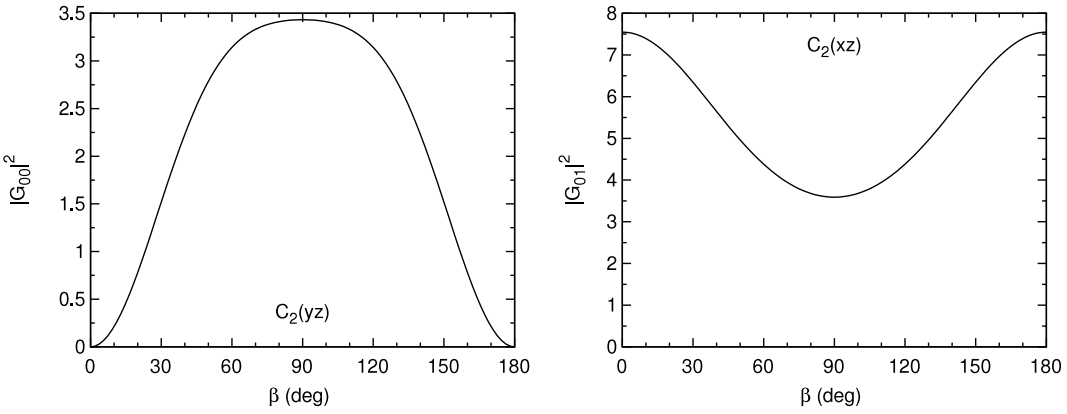

Graph 5. Orientation dependence of the structure factor squared for C_2.

Table 6
Structure coefficients for N_2.

Orbital	R	E	μ	Fit
$1\sigma_g^2 1\sigma_u^2 2\sigma_g^2 2\sigma_u^2 3\sigma_g^2 1\pi_u^4, X^1\Sigma_g^+$	2.0743	−0.6344951	0	A

2nd highest in HF calc.

l	$C_{00}^{(l)}$	l	$C_{00}^{(l)}$
0	4.993	6	7.839[−4]
2	1.699	8	7.773[−6]

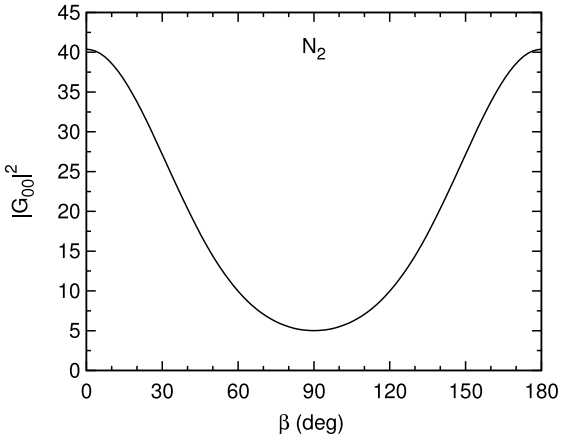

Graph 6. Orientation dependence of the structure factor squared for N_2.

Table 7
Structure coefficients for O_2.

Orbital	R	E	μ	Fit
$1\sigma_g^2 1\sigma_u^2 2\sigma_g^2 2\sigma_u^2 3\sigma_g^2 1\pi_u^4 1\underline{\pi_g^2}$, $X^3\Sigma_g^-$	2.2819	−0.5323543	0	A

(yz) state				(xz) state			
l	$C_{00}^{(l)}$	l	$C_{00}^{(l)}$	l	$C_{01}^{(l)}$	l	$C_{01}^{(l)}$
2	1.444	8	4.314[−6]	1	2.320	7	8.343[−6]
4	6.063[−2]	10	−1.511[−7]	3	1.071[−1]	9	2.725[−7]
6	7.795[−4]			5	1.423[−3]		

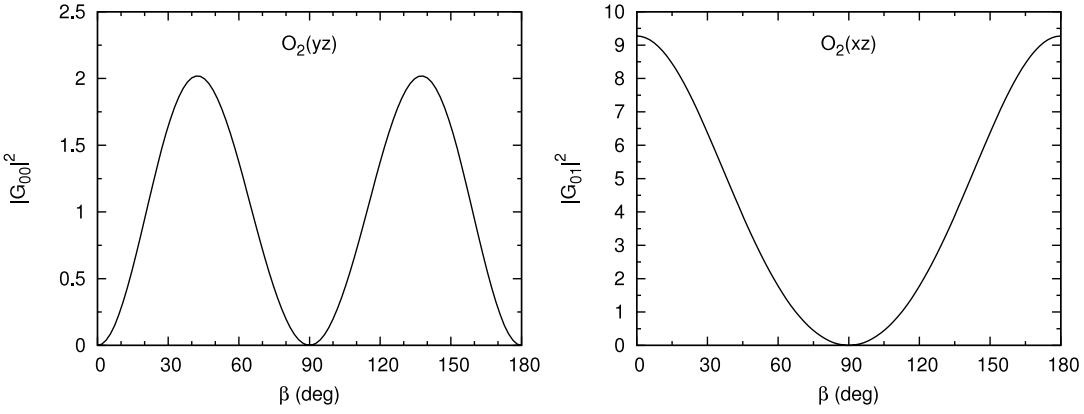

Graph 7. Orientation dependence of the structure factor squared for O_2.

Table 8
Structure coefficients for F_2.

Orbital	R	E	μ	Fit
$1\sigma_g^2 1\sigma_u^2 2\sigma_g^2 2\sigma_u^2 3\sigma_g^2 1\pi_u^4 1\pi_g^4$, $X^1\Sigma_g^+$	2.6682	−0.6669517	0	B

(yz) state				(xz) state			
l	$C_{00}^{(l)}$	l	$C_{00}^{(l)}$	l	$C_{01}^{(l)}$	l	$C_{01}^{(l)}$
2	2.354	8	−1.058[−5]	1	3.669	7	−2.783[−4]
4	1.888[−1]	10	−2.598[−6]	3	3.188[−1]	9	1.071[−3]
6	5.113[−3]			5	8.907[−3]		

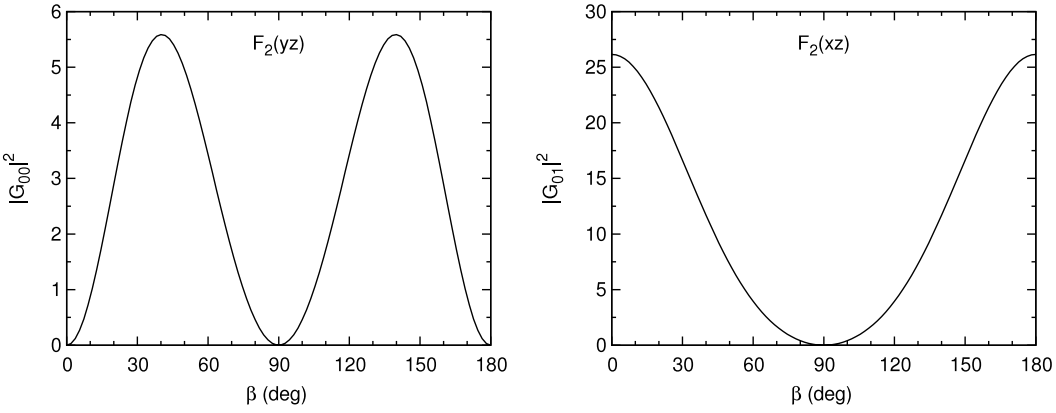

Graph 8. Orientation dependence of the structure factor squared for F_2.

Table 9
Structure coefficients for LiH.

Orbital	R	E	μ	Fit
$1\sigma^2 2\underline{\sigma^2}, X^1\Sigma^+$	3.0139	−0.3017699	−1.187618	B

l	$C_{00}^{(l)}$	l	$C_{00}^{(l)}$
0	9.838[−1]	6	−6.486[−4]
1	3.493[−1]	7	−1.162[−4]
2	5.184[−2]	8	−1.745[−5]
3	−1.224[−2]	9	−2.275[−6]
4	−9.028[−3]	10	−2.913[−7]
5	−2.877[−3]		

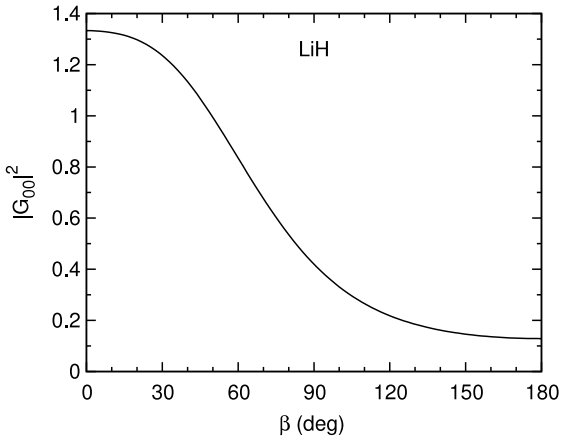

Graph 9. Orientation dependence of the structure factor squared for LiH.

Table 10
Structure coefficients for BeH.

Orbital	R	E	μ	Fit
$1\sigma^2 2\sigma^2 3\underline{\sigma}, X^2\Sigma^+$	2.5371	−0.3127291	2.657963	C

l	$C_{00}^{(l)}$	l	$C_{00}^{(l)}$
0	5.615[−1]	6	−2.062[−3]
1	8.368[−1]	7	3.842[−4]
2	−5.244[−1]	8	−5.846[−5]
3	1.673[−1]	9	7.019[−6]
4	−4.272[−2]	10	4.527[−6]
5	9.857[−3]		

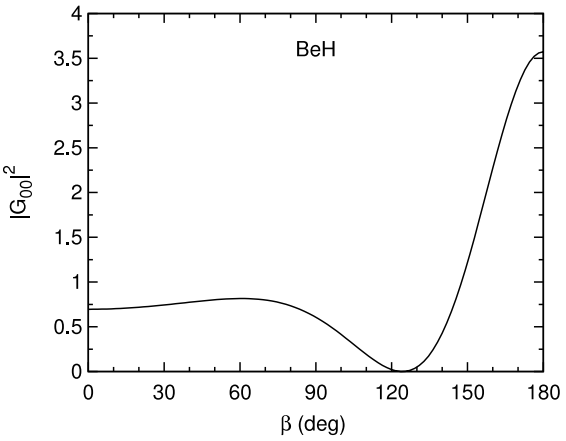

Graph 10. Orientation dependence of the structure factor squared for BeH.

Table 11
Structure coefficients for BH.

Orbital	R	E	μ	Fit
$1\sigma^2 2\sigma^2 \underline{3\sigma^2}, X^1\Sigma^+$	2.3289	−0.3483243	1.727334	B

l	$C_{00}^{(l)}$	l	$C_{00}^{(l)}$
0	3.305[−1]	6	−8.145[−4]
1	9.238[−1]	7	1.236[−4]
2	−4.521[−1]	8	−1.667[−5]
3	1.179[−1]	9	1.996[−6]
4	−2.492[−2]	10	−1.951[−7]
5	4.757[−3]		

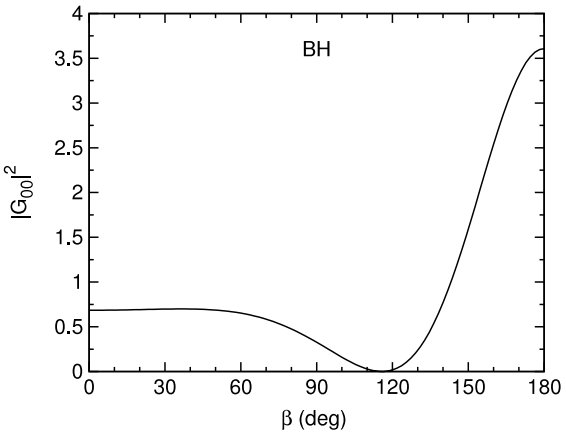

Graph 11. Orientation dependence of the structure factor squared for BH.

Table 12
Structure coefficients for CH.

Orbital	R	E	μ	Fit
$1\sigma^2 2\sigma^2 3\sigma^2 \underline{1\pi}, X^2\Pi$	2.1163	−0.4150423	9.647121[−1]	B

(yz) state				(xz) state			
l	$C_{00}^{(l)}$	l	$C_{00}^{(l)}$	l	$C_{01}^{(l)}$	l	$C_{01}^{(l)}$
1	1.780	6	−7.960[−5]	0	2.289	6	1.773[−5]
2	−1.006[−1]	7	8.997[−6]	1	−1.706[−1]	7	−1.854[−6]
3	5.527[−3]	8	−9.377[−7]	2	1.080[−2]	8	1.754[−7]
4	−3.256[−3]	9	8.053[−8]	3	−6.176[−3]	9	−1.823[−8]
5	6.229[−4]	10	−9.529[−9]	4	1.200[−3]	10	3.742[−9]
				5	−1.555[−4]		

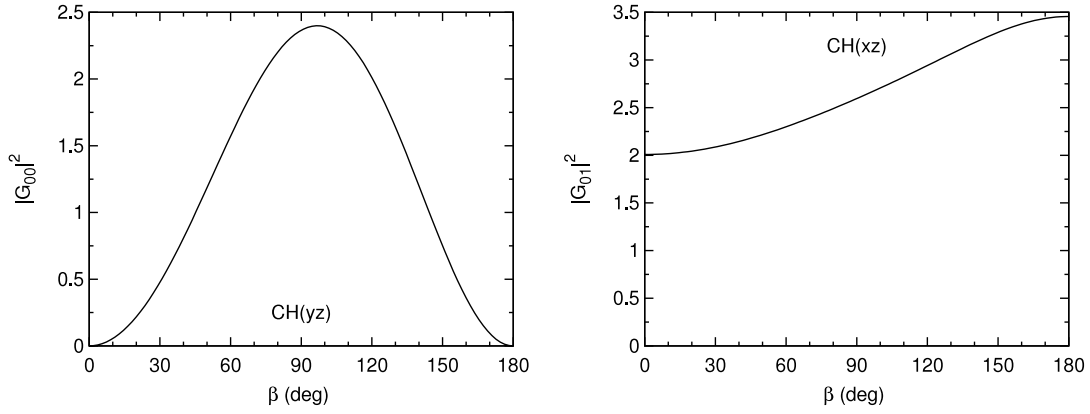

Graph 12. Orientation dependence of the structure factor squared for CH.

Table 13
Structure coefficients for NH.

Orbital	R	E	μ	Fit
$1\sigma^2 2\sigma^2 3\sigma^2 \underline{1\pi^2}, X^3\Sigma^-$	1.9582	−0.5380064	9.112619[−1]	B

(yz) state				(xz) state			
l	$C_{00}^{(l)}$	l	$C_{00}^{(l)}$	l	$C_{01}^{(l)}$	l	$C_{01}^{(l)}$
1	2.339	6	−1.585[−4]	0	2.830	6	3.665[−5]
2	−1.500[−1]	7	1.969[−5]	1	−2.403[−1]	7	−4.207[−6]
3	1.976[−2]	8	−2.231[−6]	2	3.469[−2]	8	5.075[−7]
4	−6.299[−3]	9	2.407[−7]	3	−1.121[−2]	9	−8.248[−8]
5	1.139[−3]	10	−2.462[−8]	4	2.064[−3]	10	3.859[−8]
				5	−2.910[−4]		

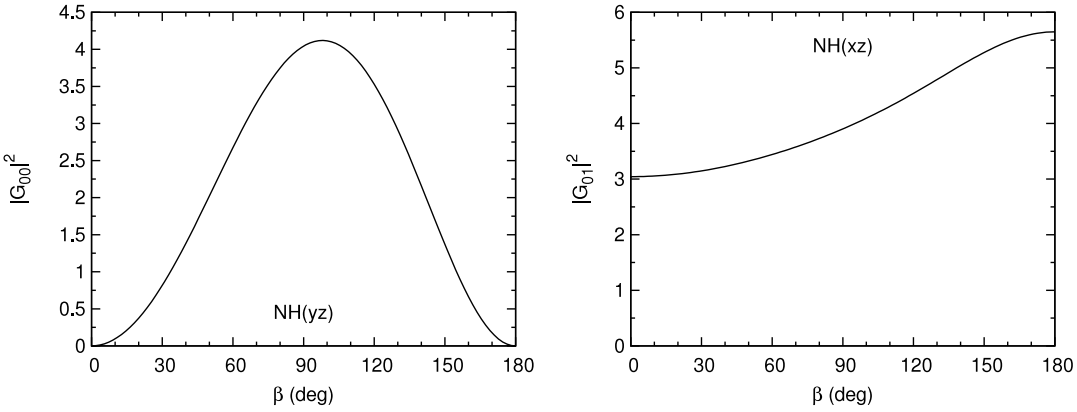

Graph 13. Orientation dependence of the structure factor squared for NH.

Table 14
Structure coefficients for OH.

Orbital	R	E	μ	Fit
$1\sigma^2 2\sigma^2 3\sigma^2 \underline{1\pi^3}$, $X^2\Pi$	1.8324	−0.5725469	8.574762[−1]	B

(yz) state				(xz) state			
l	$C_{00}^{(l)}$	l	$C_{00}^{(l)}$	l	$C_{01}^{(l)}$	l	$C_{01}^{(l)}$
1	2.119	6	−1.743[−4]	0	2.537	6	3.894[−5]
2	−1.886[−1]	7	2.135[−5]	1	−2.970[−1]	7	−4.395[−6]
3	3.894[−2]	8	−2.311[−6]	2	6.585[−2]	8	4.700[−7]
4	−7.772[−3]	9	2.464[−7]	3	−1.357[−2]	9	−1.087[−7]
5	1.259[−3]	10	−8.597[−8]	4	2.240[−3]	10	8.088[−8]
				5	−3.143[−4]		

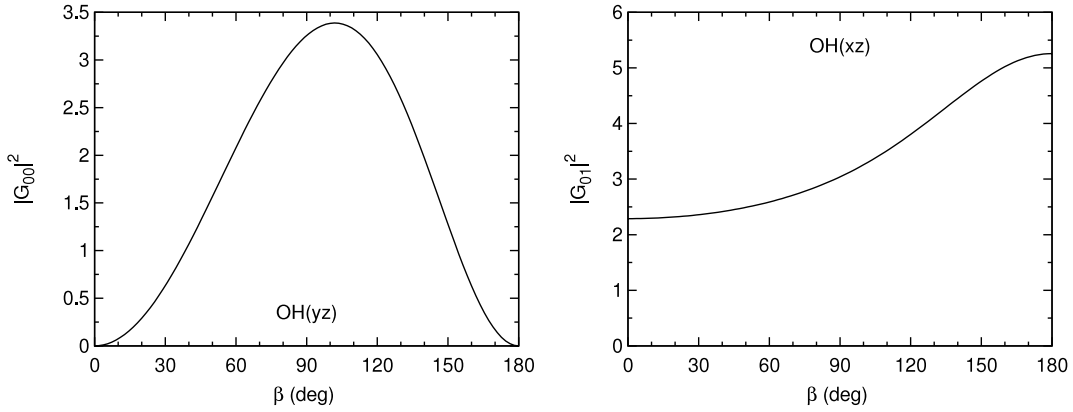

Graph 14. Orientation dependence of the structure factor squared for OH.

Table 15
Structure coefficients for HF.

Orbital	R	E	μ	Fit
$1\sigma^2 2\sigma^2 3\sigma^2 \underline{1\pi^4}, X^1\Sigma^+$	1.7325	−0.6504098	−8.179481[−1]	B

(yz) state				(xz) state			
l	$C_{00}^{(l)}$	l	$C_{00}^{(l)}$	l	$C_{01}^{(l)}$	l	$C_{01}^{(l)}$
1	2.226	6	2.204[−4]	0	2.589	6	4.709[−5]
2	2.271[−1]	7	2.723[−5]	1	3.467[−1]	7	4.982[−6]
3	5.215[−2]	8	2.969[−6]	2	8.537[−2]	8	−7.999[−8]
4	9.748[−3]	9	3.027[−7]	3	1.649[−2]	9	6.360[−8]
5	1.576[−3]	10	−8.908[−8]	4	2.719[−3]	10	−8.434[−8]
				5	3.847[−4]		

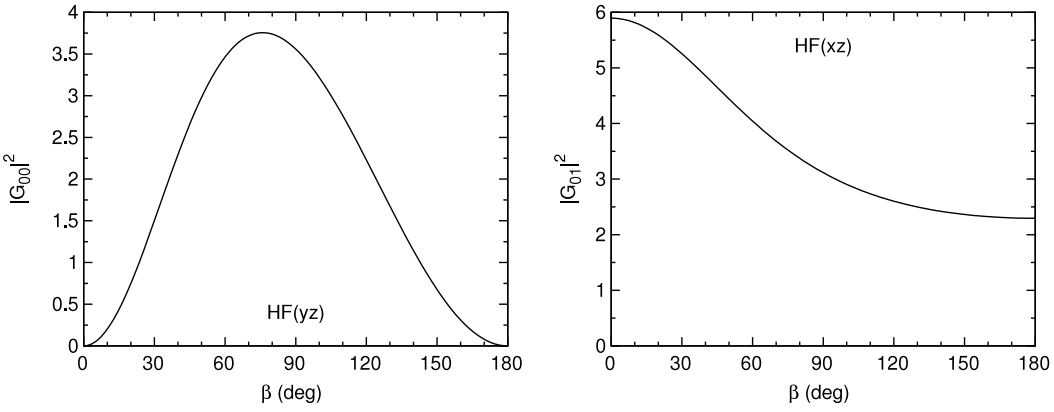

Graph 15. Orientation dependence of the structure factor squared for HF.

Table 16
Structure coefficients for NaH.

Orbital	R	E	μ	Fit
$1\sigma^2 2\sigma^2 1\pi^4 3\sigma^2 \underline{4\sigma^2}$, $X^1\Sigma^+$	3.5667	−0.2754223	−1.398163	B

l	$C_{00}^{(l)}$	l	$C_{00}^{(l)}$
0	1.064	6	7.144[−4]
1	5.974[−1]	7	1.266[−4]
2	2.321[−1]	8	2.014[−5]
3	6.785[−2]	9	2.729[−6]
4	1.675[−2]	10	9.466[−8]
5	3.646[−3]		

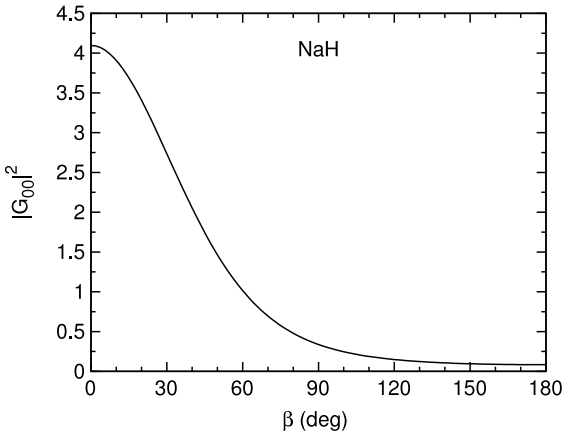

Graph 16. Orientation dependence of the structure factor squared for NaH.

Table 17
Structure coefficients for MgH.

Orbital	R	E	μ	Fit
$1\sigma^2 2\sigma^2 1\pi^4 3\sigma^2 4\sigma^2 \underline{5\sigma}, X^2\Sigma^+$	3.2687	−0.2598007	3.190913	C

l	$C_{00}^{(l)}$	l	$C_{00}^{(l)}$
0	4.271[−1]	6	−3.062[−3]
1	8.837[−1]	7	6.258[−4]
2	−5.571[−1]	8	−2.486[−5]
3	1.888[−1]	9	6.676[−6]
4	−5.289[−2]	10	7.211[−5]
5	1.350[−2]		

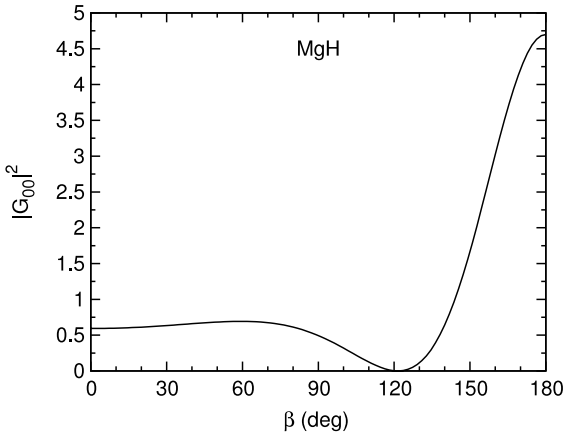

Graph 17. Orientation dependence of the structure factor squared for MgH.

Table 18
Structure coefficients for AlH.

Orbital	R	E	μ	Fit
$1\sigma^2 2\sigma^2 1\pi^4 3\sigma^2 4\sigma^2 \underline{5\sigma^2}$, $X^1\Sigma^+$	3.1139	−0.2890256	1.938848	B

l	$C_{00}^{(l)}$	l	$C_{00}^{(l)}$
0	4.218[−1]	6	−8.212[−4]
1	9.354[−1]	7	1.345[−4]
2	−3.742[−1]	8	−1.938[−5]
3	8.954[−2]	9	2.635[−6]
4	−2.030[−2]	10	−2.586[−7]
5	4.359[−3]		

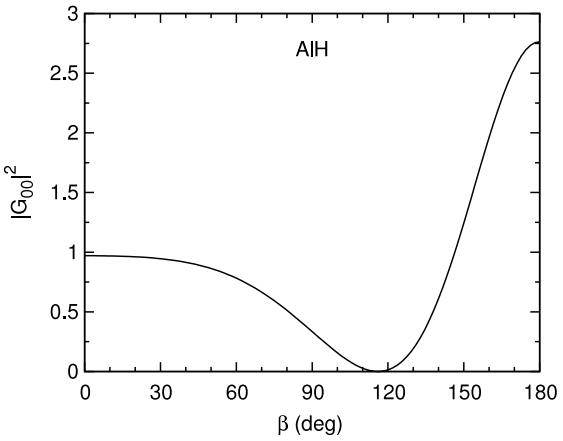

Graph 18. Orientation dependence of the structure factor squared for AlH.

Table 19
Structure coefficients for SiH.

Orbital	R	E	μ	Fit
$1\sigma^2 2\sigma^2 1\pi^4 3\sigma^2 4\sigma^2 5\sigma^2 \underline{2\pi}$, $X^2\Pi$	2.8726	−0.2863864	1.382779	B

(yz) state				(xz) state			
l	$C_{00}^{(l)}$	l	$C_{00}^{(l)}$	l	$C_{01}^{(l)}$	l	$C_{01}^{(l)}$
1	1.383	6	−5.908[−5]	0	1.933	6	1.407[−5]
2	6.372[−3]	7	6.535[−6]	1	1.007[−2]	7	−1.579[−6]
3	−1.646[−2]	8	−7.249[−7]	2	−3.166[−2]	8	1.726[−7]
4	−1.050[−3]	9	7.962[−8]	3	−2.241[−3]	9	−1.377[−8]
5	4.599[−4]	10	−2.643[−9]	4	9.685[−4]	10	3.104[−9]
				5	−1.264[−4]		

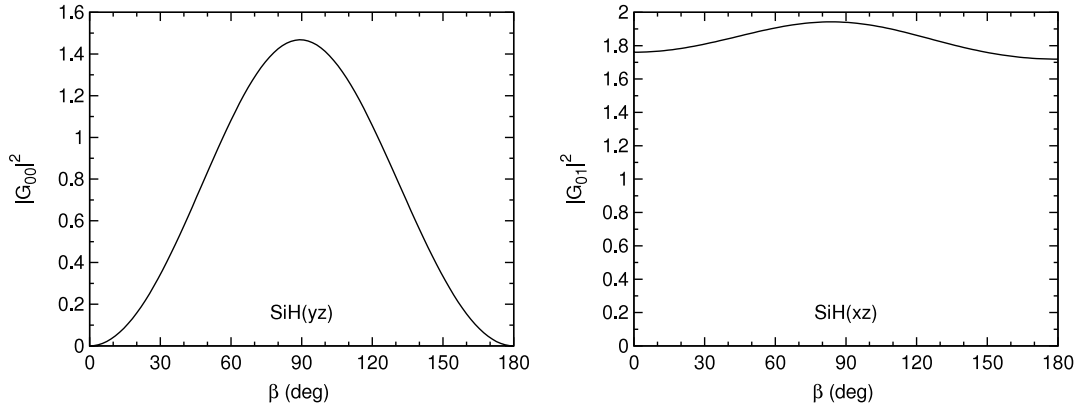

Graph 19. Orientation dependence of the structure factor squared for SiH.

Table 20
Structure coefficients for PH.

Orbital	R	E	μ	Fit
$1\sigma^2 2\sigma^2 3\sigma^2 1\pi^4 4\sigma^2 5\sigma^2 \underline{2\pi}^2$, $X^3\Sigma^-$	2.6878	−0.3789867	1.284812	B

(yz) state				(xz) state			
l	$C_{00}^{(l)}$	l	$C_{00}^{(l)}$	l	$C_{01}^{(l)}$	l	$C_{01}^{(l)}$
1	2.259	6	−1.620[−4]	0	2.957	6	4.422[−5]
2	−1.965[−2]	7	2.182[−5]	1	−3.855[−2]	7	−5.619[−6]
3	−1.099[−2]	8	−2.763[−6]	2	−1.867[−2]	8	6.518[−7]
4	−4.118[−3]	9	3.016[−7]	3	−8.076[−3]	9	−8.148[−8]
5	1.087[−3]	10	−3.868[−8]	4	2.149[−3]	10	2.039[−8]
				5	−3.243[−4]		

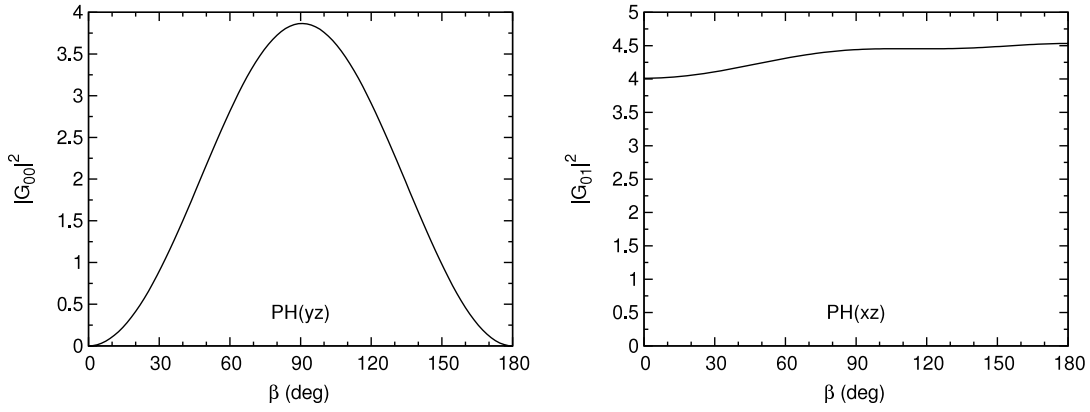

Graph 20. Orientation dependence of the structure factor squared for PH.

Table 21
Structure coefficients for SH.

Orbital	R	E	μ	Fit
$1\sigma^2 2\sigma^2 3\sigma^2 1\pi^4 4\sigma^2 5\sigma^2 \underline{2\pi^3}, X^2\Pi$	2.5339	−0.4130085	1.202995	B

(yz) state				(xz) state			
l	$C_{00}^{(l)}$	l	$C_{00}^{(l)}$	l	$C_{01}^{(l)}$	l	$C_{01}^{(l)}$
1	2.183	6	−2.087[−4]	0	2.825	6	5.808[−5]
2	−6.729[−2]	7	2.927[−5]	1	−1.195[−1]	7	−7.373[−6]
3	2.372[−2]	8	−3.694[−6]	2	4.443[−2]	8	8.888[−7]
4	−6.239[−3]	9	4.032[−7]	3	−1.194[−2]	9	−1.312[−7]
5	1.282[−3]	10	−5.967[−8]	4	2.490[−3]	10	4.636[−8]
				5	−4.100[−4]		

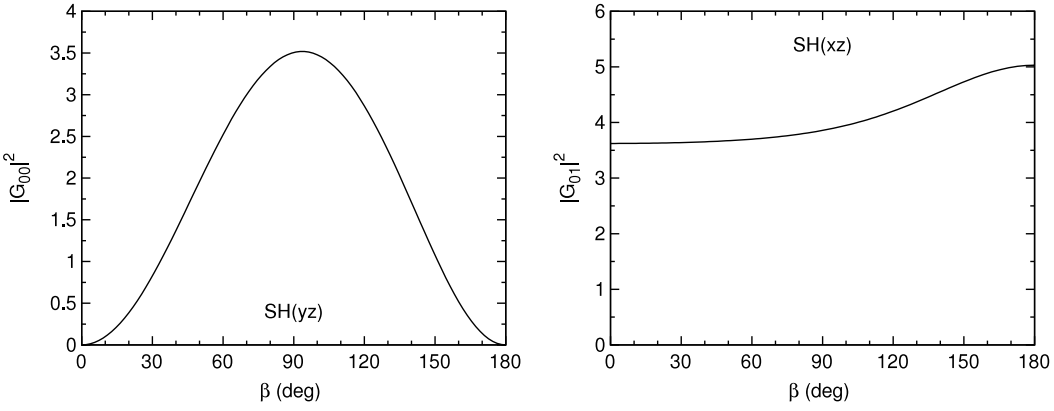

Graph 21. Orientation dependence of the structure factor squared for SH.

Table 22
Structure coefficients for HCl.

Orbital	R	E	μ	Fit
$1\sigma^2 2\sigma^2 3\sigma^2 1\pi^4 4\sigma^2 5\sigma^2 \underline{2\pi}^4$, $X\ ^1\Sigma^+$	2.4086	−0.4770277	−1.142830	B

(yz) state				(xz) state			
l	$C_{00}^{(l)}$	l	$C_{00}^{(l)}$	l	$C_{01}^{(l)}$	l	$C_{01}^{(l)}$
1	2.507	6	3.331[−4]	0	3.147	6	9.426[−5]
2	1.232[−1]	7	4.854[−5]	1	2.094[−1]	7	1.314[−5]
3	4.838[−2]	8	6.483[−6]	2	8.645[−2]	8	2.205[−6]
4	1.005[−2]	9	8.793[−7]	3	1.856[−2]	9	4.203[−7]
5	2.015[−3]	10	1.321[−7]	4	3.782[−3]	10	9.889[−8]
				5	6.332[−4]		

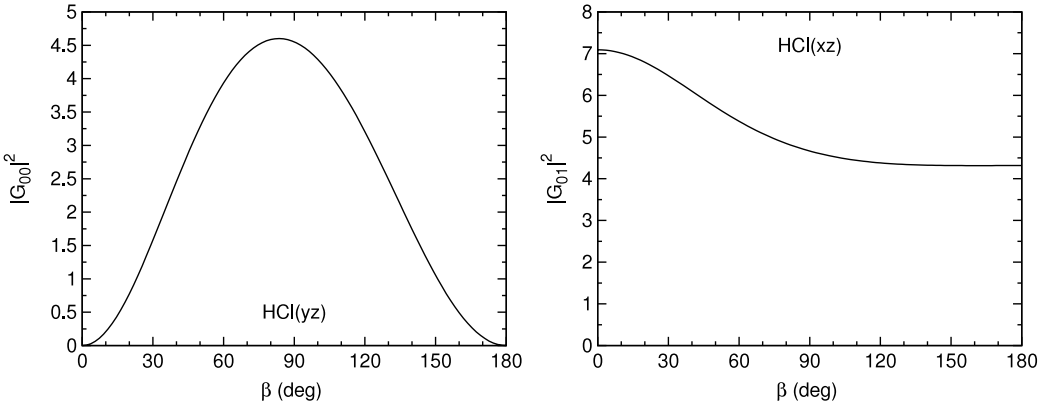

Graph 22. Orientation dependence of the structure factor squared for HCl.

Table 23
Structure coefficients for LiB.

Orbital	R	E	μ	Fit
$1\sigma^2 2\sigma^2 3\sigma^2 \underline{4\sigma^2}$,$^1\Sigma^+$ ($^3\Pi$ in Exp)	4.5274	−0.2026138	−1.597511	B

l	$C_{00}^{(l)}$	l	$C_{00}^{(l)}$
0	3.773[−1]	6	2.877[−4]
1	6.030[−1]	7	3.008[−5]
2	1.951[−1]	8	2.920[−6]
3	5.528[−2]	9	4.053[−7]
4	1.230[−2]	10	1.695[−6]
5	2.115[−3]		

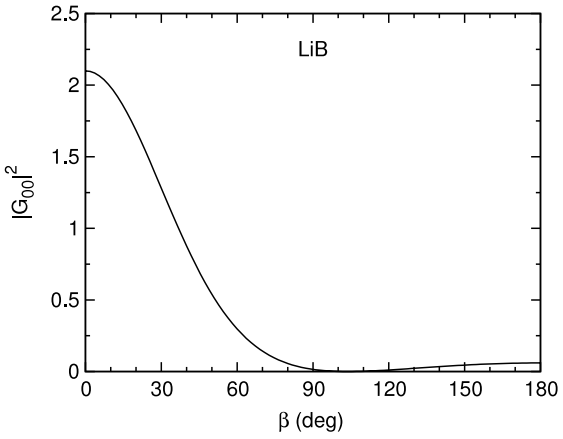

Graph 23. Orientation dependence of the structure factor squared for LiB.

Table 24
Structure coefficients for BeB.

Orbital	R	E	μ	Fit
$1\sigma^2 2\sigma^2 3\sigma^2 \underline{4\sigma^2} 1\pi\ ,^2\Pi$	4 (repulsive in HF)	−0.2911527	5.929580[−1]	B

N/A in CCCBDB[37]

l	$C_{00}^{(l)}$	l	$C_{00}^{(l)}$
0	3.507[−1]	6	−6.942[−4]
1	1.545	7	9.997[−5]
2	−1.820[−1]	8	−1.311[−5]
3	1.498[−1]	9	3.052[−6]
4	−2.149[−2]	10	−3.604[−6]
5	5.340[−3]		

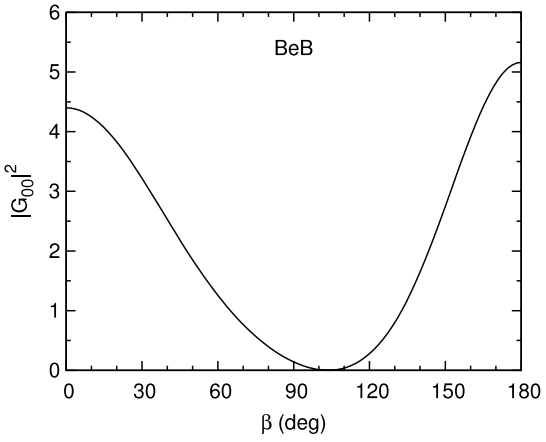

Graph 24. Orientation dependence of the structure factor squared for BeB.

Table 25
Structure coefficients for LiC.

Orbital	R	E	μ	Fit
$1\sigma^2 2\sigma^2 3\sigma^2 1\pi \underline{4\sigma^2}$, $^2\Pi$ ($^4\Sigma$ in exp)	3.8865 (HF)	−0.2522427	−1.777516	B

l	$C_{00}^{(l)}$	l	$C_{00}^{(l)}$
0	3.998[−1]	6	−6.808[−4]
1	6.655[−1]	7	−1.917[−4]
2	2.123[−1]	8	−4.033[−5]
3	4.232[−2]	9	−7.213[−6]
4	3.246[−3]	10	−2.524[−7]
5	−1.312[−3]		

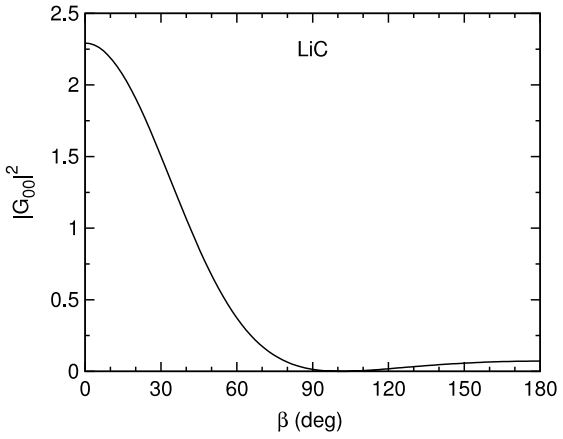

Graph 25. Orientation dependence of the structure factor squared for LiC.

Table 26
Structure coefficients for BeC.

Orbital	R	E	μ	Fit
$1\sigma^2 2\sigma^2 3\sigma^2 1\pi^2 \underline{4\sigma^2}\,,^3\Sigma^-$	3.2607 (HF)	−0.3185210	−1.314343[−1]	B

N/A in CCCBDB[37]

l	$C_{00}^{(l)}$	l	$C_{00}^{(l)}$
0	9.359[−1]	6	2.944[−4]
1	1.644	7	4.226[−5]
2	2.805[−1]	8	1.829[−6]
3	1.329[−1]	9	1.126[−6]
4	1.480[−2]	10	−1.062[−6]
5	3.372[−3]		

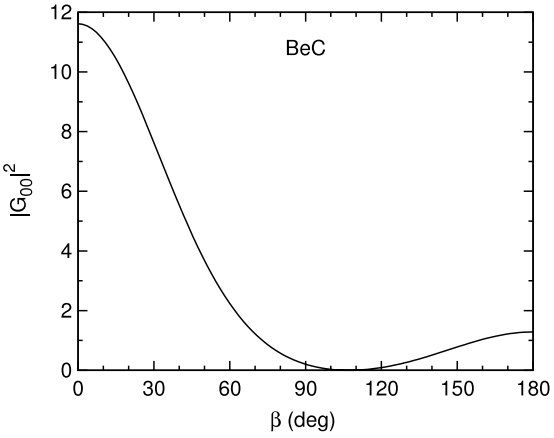

Graph 26. Orientation dependence of the structure factor squared for BeC.

Table 27
Structure coefficients for LiN.

Orbital	R	E	μ	Fit
$1\sigma^2 2\sigma^2 3\sigma^2 1\pi^2 4\underline{\sigma^2}\,,^3\Sigma^-$	3.4783 (HF)	−0.3.096106	−1.694672	B

l	$C_{00}^{(l)}$	l	$C_{00}^{(l)}$
0	2.968[−1]	6	−2.414[−3]
1	6.012[−1]	7	−5.576[−4]
2	1.190[−1]	8	−1.073[−4]
3	−1.332[−2]	9	−1.805[−5]
4	−1.928[−2]	10	−2.433[−6]
5	−8.246[−3]		

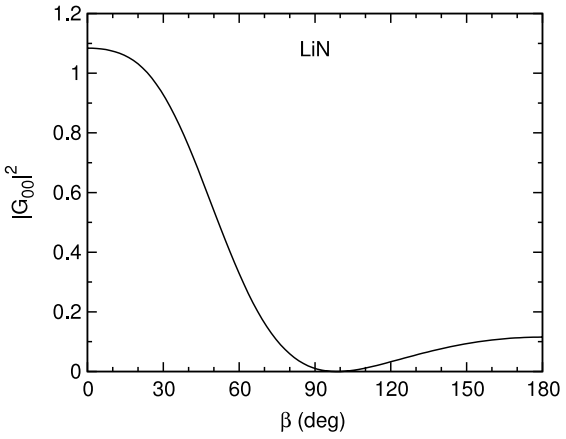

Graph 27. Orientation dependence of the structure factor squared for LiN.

Table 28
Structure coefficients for BeN.

Orbital	R	E	μ	Fit
$1\sigma^2 2\sigma^2 3\sigma^2 4\sigma^2 \underline{1\pi^3}$,$^2\Pi$ ($^4\Sigma$ in exp)	2.6948 (HF)	−0.3894105	−1.273005	B

(yz) state				(xz) state			
l	$C_{00}^{(l)}$	l	$C_{00}^{(l)}$	l	$C_{01}^{(l)}$	l	$C_{01}^{(l)}$
1	1.494	6	2.545[−3]	0	2.214	6	7.926[−4]
2	6.439[−1]	7	3.837[−4]	1	1.199	7	1.044[−4]
3	2.464[−1]	8	5.026[−5]	2	4.812[−1]	8	1.206[−5]
4	6.659[−2]	9	5.727[−6]	3	1.332[−1]	9	1.257[−6]
5	1.434[−2]	10	6.211[−7]	4	2.910[−2]	10	9.998[−8]
				5	5.217[−3]		

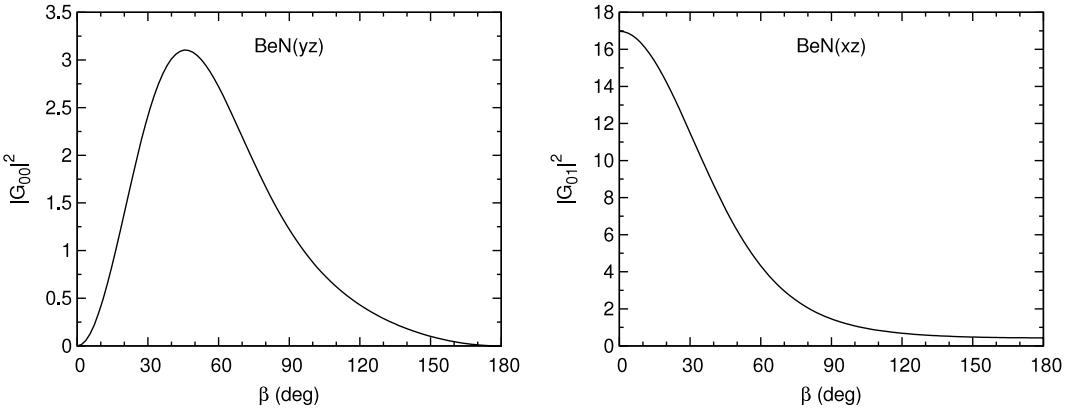

Graph 28. Orientation dependence of the structure factor squared for BeN.

Table 29
Structure coefficients for BN.

Orbital	R	E	μ	Fit
$1\sigma^2 2\sigma^2 3\sigma^2 4\sigma^2 1\pi^2 \underline{5\sigma^2}$,$^3\Sigma$ ($^3\Pi$ in exp)	2.5039	−0.3723203	2.022762	B

l	$C_{00}^{(l)}$	l	$C_{00}^{(l)}$
0	1.782	6	4.800[−3]
1	−4.940[−1]	7	−9.493[−4]
2	2.456[−1]	8	1.620[−4]
3	−1.620[−1]	9	−2.422[−5]
4	6.795[−2]	10	2.994[−6]
5	−2.031[−2]		

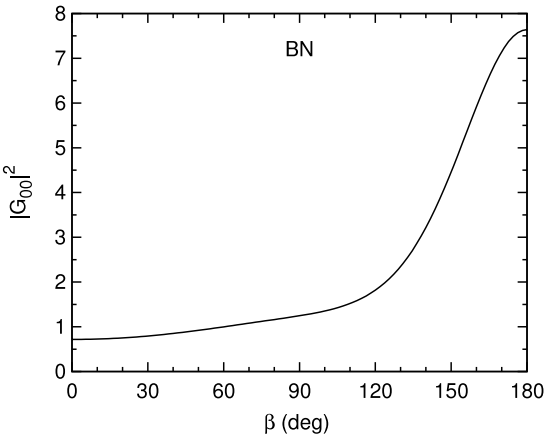

Graph 29. Orientation dependence of the structure factor squared for BN.

Table 30
Structure coefficients for CN.

Orbital	R	E	μ	Fit
$1\sigma^2 2\sigma^2 3\sigma^2 4\sigma^2 5\sigma \underline{1\pi^4}, X^2\Sigma^+$	2.2144	−0.5124793	−1.302898[−1]	B

(yz) state				(xz) state			
l	$C_{00}^{(l)}$	l	$C_{00}^{(l)}$	l	$C_{01}^{(l)}$	l	$C_{01}^{(l)}$
1	2.675	6	4.969[−4]	0	3.428	6	1.058[−4]
2	3.787[−1]	7	5.875[−5]	1	6.253[−1]	7	7.939[−6]
3	2.200[−1]	8	4.264[−6]	2	3.805[−1]	8	5.088[−7]
4	2.556[−2]	9	2.346[−6]	3	4.580[−2]	9	−2.485[−6]
5	5.167[−3]	10	−7.567[−7]	4	9.411[−3]	10	−3.818[−6]
				5	9.136[−4]		

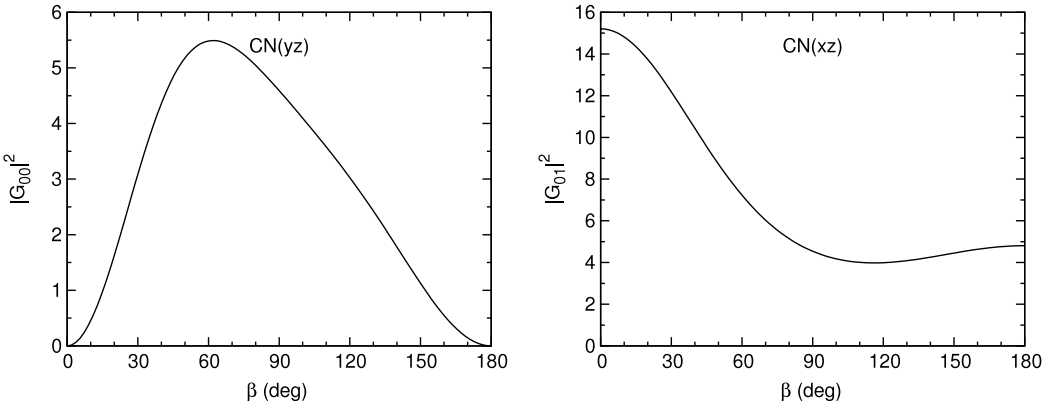

Graph 30. Orientation dependence of the structure factor squared for CN.

Table 31
Structure coefficients for LiO.

Orbital	R	E	μ	Fit
$1\sigma^2 2\sigma^2 3\sigma^2 4\sigma \underline{1\pi^4}\,,^2\,\Sigma$	3.1903	−0.3867705	−1.494245	B

(yz) state				(xz) state			
l	$C_{00}^{(l)}$	l	$C_{00}^{(l)}$	l	$C_{01}^{(l)}$	l	$C_{01}^{(l)}$
1	1.165	6	2.311[−3]	0	1.652	6	8.722[−4]
2	4.138[−1]	7	4.280[−4]	1	7.548[−1]	7	1.453[−4]
3	1.514[−1]	8	7.048[−5]	2	2.919[−1]	8	2.236[−5]
4	4.417[−2]	9	1.009[−5]	3	8.729[−2]	9	3.606[−6]
5	1.090[−2]	10	1.446[−6]	4	2.183[−2]	10	7.214[−7]
				5	4.669[−3]		

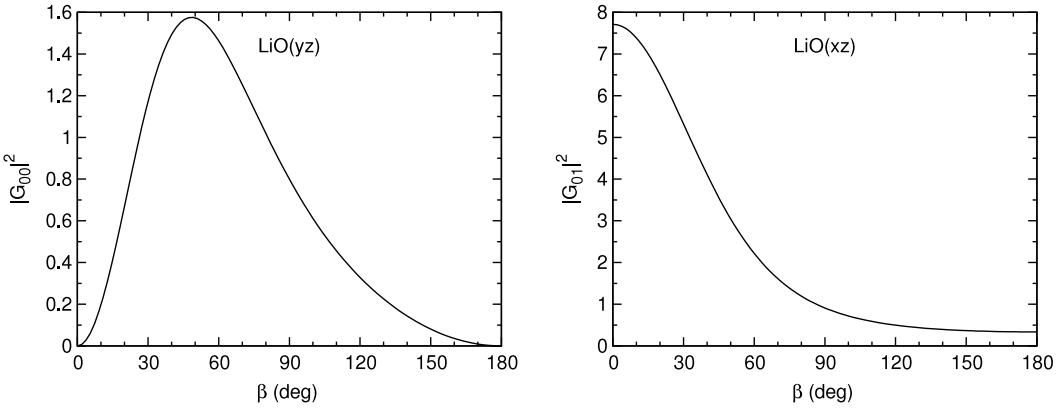

Graph 31. Orientation dependence of the structure factor squared for LiO.

Table 32
Structure coefficients for BeO.

Orbital	R	E	μ	Fit
$1\sigma^2 2\sigma^2 3\sigma^2 4\sigma^2 \underline{1\pi^4}, X^1\Sigma^+$	2.5150	−0.3885159	−8.578312[−1]	B

(yz) state				(xz) state			
l	$C_{00}^{(l)}$	l	$C_{00}^{(l)}$	l	$C_{01}^{(l)}$	l	$C_{01}^{(l)}$
1	1.532	6	3.280[−3]	0	2.236	6	1.048[−3]
2	7.122[−1]	7	5.175[−4]	1	1.300	7	1.447[−4]
3	2.773[−1]	8	7.080[−5]	2	5.304[−1]	8	1.774[−5]
4	7.842[−2]	9	8.725[−6]	3	1.535[−1]	9	1.658[−6]
5	1.765[−2]	10	9.230[−7]	4	3.502[−2]	10	−1.373[−6]
				5	6.572[−3]		

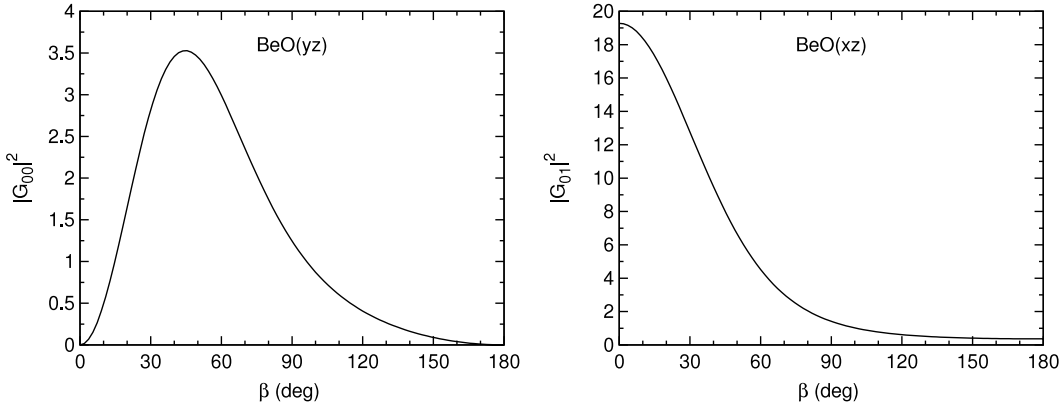

Graph 32. Orientation dependence of the structure factor squared for BeO.

Table 33
Structure coefficients for BO.

Orbital	R	E	μ	Fit
$1\sigma^2 2\sigma^2 3\sigma^2 4\sigma^2 \underline{1\pi}^4 5\sigma\,, X^2\Sigma^+$	2.2762	−0.5251085	−6.955553[−1]	B

(yz) state				(xz) state			
l	$C_{00}^{(l)}$	l	$C_{00}^{(l)}$	l	$C_{01}^{(l)}$	l	$C_{01}^{(l)}$
1	2.661	6	3.850[−3]	0	3.484	6	1.201[−3]
2	8.170[−1]	7	6.339[−4]	1	1.383	7	1.800[−4]
3	3.365[−1]	8	8.854[−5]	2	5.955[−1]	8	2.284[−5]
4	9.022[−2]	9	1.21977[−5]	3	1.639[−1]	9	1.125[−5]
5	2.033[−2]	10	2.19513[−7]	4	3.747[−2]	10	6.747[−6]
				5	7.175[−3]		

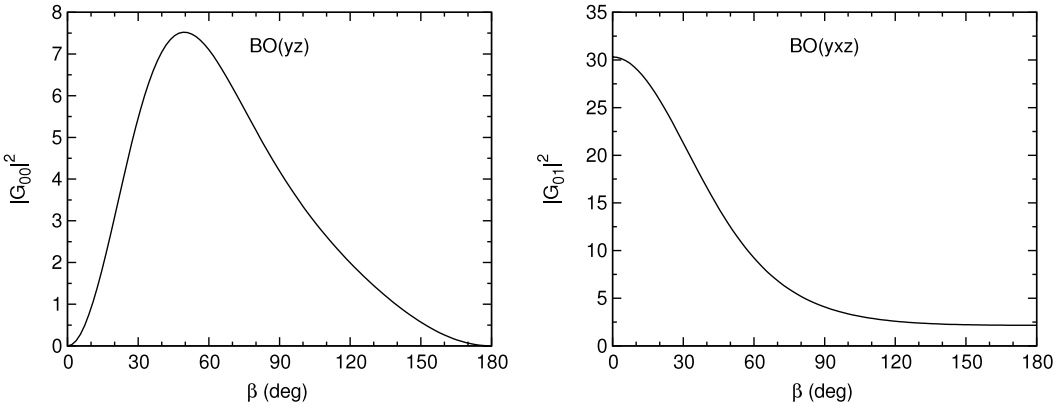

Graph 33. Orientation dependence of the structure factor squared for BO.

Table 34
Structure coefficients for CO.

Orbital	R	E	μ	Fit
$1\sigma^2 2\sigma^2 3\sigma^2 4\sigma^2 1\pi^4 \underline{5\sigma^2}$, $X^1\Sigma^+$	2.1320	−0.5549234	1.565339	B

l	$C_{00}^{(l)}$	l	$C_{00}^{(l)}$
0	3.346	6	1.130[−2]
1	−1.003	7	−2.275[−3]
2	8.215[−1]	8	3.993[−4]
3	−4.584[−1]	9	−6.197[−5]
4	1.688[−1]	10	8.100[−6]
5	−4.802[−2]		

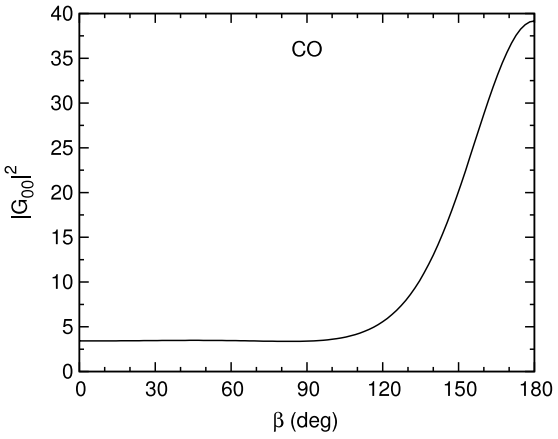

Graph 34. Orientation dependence of the structure factor squared for CO.

Table 35
Structure coefficients for NO.

Orbital	R	E	μ	Fit
$1\sigma^2 2\sigma^2 3\sigma^2 4\sigma^2 5\sigma^2 1\pi^4 \underline{2\pi}, X^2\Pi$	2.1747	−0.4117863	4.618554[−1]	C

(yz) state				(xz) state			
l	$C_{00}^{(l)}$	l	$C_{00}^{(l)}$	l	$C_{01}^{(l)}$	l	$C_{01}^{(l)}$
1	2.284[−1]	6	5.189[−4]	0	1.970[−1]	6	−1.043[−4]
2	8.543[−1]	7	−4.199[−5]	1	1.457	7	1.469[−6]
3	−1.117[−1]	8	−4.624[−5]	2	−2.070[−1]	8	1.445[−6]
4	3.070[−2]	9	1.587[−5]	3	5.795[−2]	9	−8.669[−7]
5	−4.250[−3]	10	−4.039[−5]	4	−8.231[−3]	10	−6.435[−8]
				5	1.034[−3]		

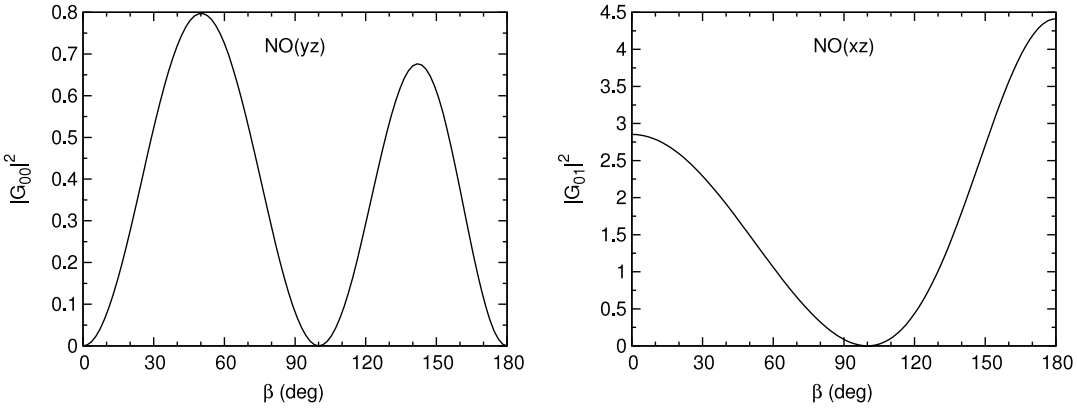

Graph 35. Orientation dependence of the structure factor squared for NO.

Table 36
Structure coefficients for LiF.

Orbital	R	E	μ	Fit
$1\sigma^2 2\sigma^2 3\sigma^2 4\sigma^2 \underline{1\pi^4}, X^1\Sigma^+$	2.9553	−0.4761263	−1.411108	B

(yz) state				(xz) state			
l	$C_{00}^{(l)}$	l	$C_{00}^{(l)}$	l	$C_{01}^{(l)}$	l	$C_{01}^{(l)}$
1	1.417	6	2.302[−3]	0	1.886	6	8.224[−4]
2	4.697[−1]	7	4.259[−4]	1	8.070[−1]	7	1.365[−4]
3	1.594[−1]	8	7.035[−5]	2	2.910[−1]	8	2.030[−5]
4	4.529[−2]	9	1.036[−5]	3	8.488[−2]	9	2.805[−6]
5	1.096[−2]	10	1.499[−6]	4	2.085[−2]	10	3.130[−7]
				5	4.419[−3]		

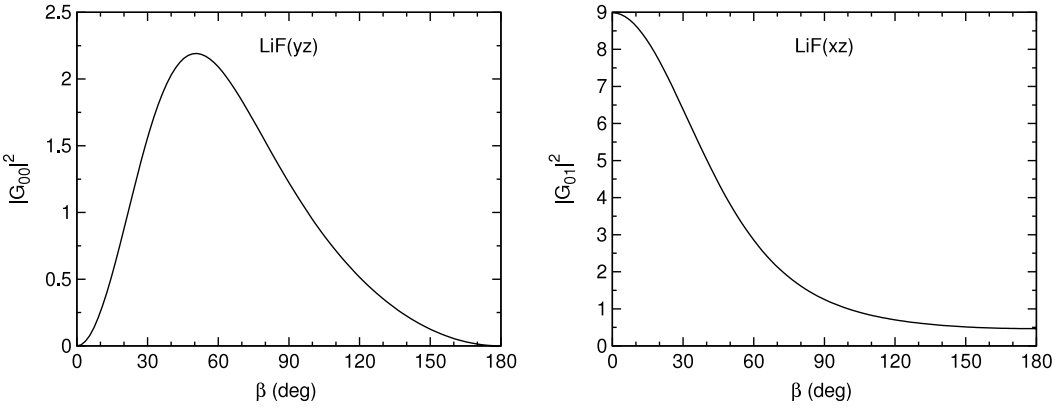

Graph 36. Orientation dependence of the structure factor squared for LiF.

Table 37
Structure coefficients for BeF.

Orbital	R	E	μ	Fit
$1\sigma^2 2\sigma^2 3\sigma^2 4\sigma^2 1\pi^4 \underline{5\sigma}, X^2\Sigma^+$	2.5719	−0.3380721	2.615925	B

l	$C_{00}^{(l)}$	l	$C_{00}^{(l)}$
0	1.570	6	1.202[−3]
1	2.099[−2]	7	−2.649[−4]
2	−9.756[−2]	8	5.145[−5]
3	−4.118[−3]	9	−8.901[−6]
4	1.189[−2]	10	1.424[−6]
5	−4.553[−3]		

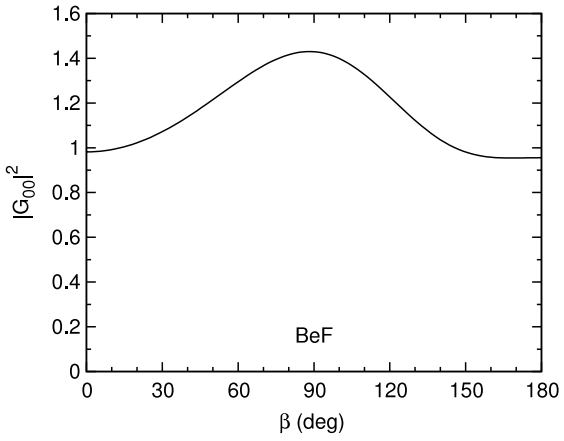

Graph 37. Orientation dependence of the structure factor squared for BeF.

Table 38
Structure coefficients for BF.

Orbital	R	E	μ	Fit
$1\sigma^2 2\sigma^2 3\sigma^2 4\sigma^2 1\pi^4 \underline{5\sigma^2}$, $X^1\Sigma^+$	2.3940	−0.4056581	1.986358	A

l	$C_{00}^{(l)}$	l	$C_{00}^{(l)}$
0	1.879	6	2.972[−3]
1	−2.805[−1]	7	−6.250[−4]
2	4.791[−2]	8	1.139[−4]
3	−6.787[−2]	9	−1.839[−5]
4	3.587[−2]	10	2.180[−6]
5	−1.179[−2]		

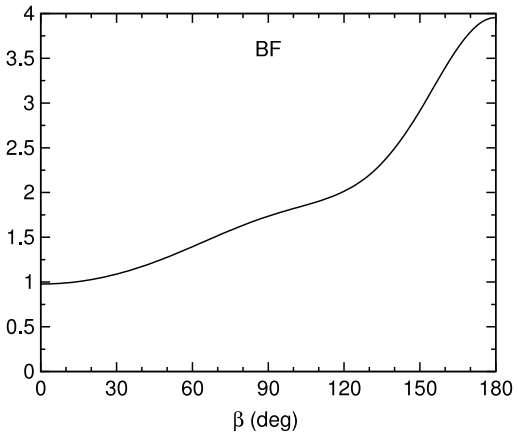

Graph 38. Orientation dependence of the structure factor squared for BF.

Table 39
Structure coefficients for CF.

Orbital	R	E	μ	Fit
$1\sigma^2 2\sigma^2 3\sigma^2 4\sigma^2 1\pi^4 5\sigma^2 \underline{2\pi}, X^2\Pi$	2.4034	−0.3903375	1.131481	C

(yz) state				(xz) state			
l	$C_{00}^{(l)}$	l	$C_{00}^{(l)}$	l	$C_{01}^{(l)}$	l	$C_{01}^{(l)}$
1	1.011	6	1.625[−3]	0	1.162	6	−4.921[−4]
2	4.601[−1]	7	−1.971[−4]	1	8.350[−1]	7	5.681[−5]
3	−1.792[−1]	8	−5.708[−5]	2	−3.415[−1]	8	−2.207[−7]
4	4.468[−2]	9	6.398[−5]	3	8.761[−2]	9	2.707[−6]
5	−9.409[−3]	10	−8.123[−5]	4	−1.878[−2]	10	−1.681[−6]
				5	3.348[−3]		

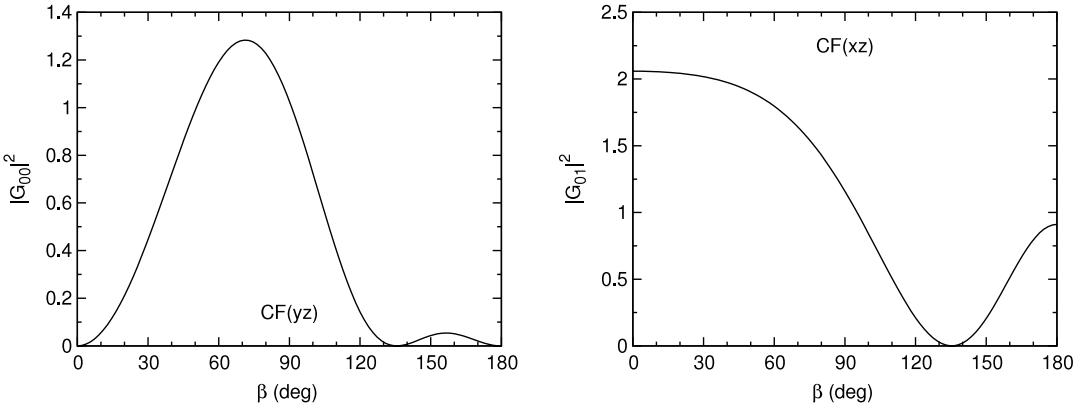

Graph 39. Orientation dependence of the structure factor squared for CF.

Table 40
Structure coefficients for NF.

Orbital	R	E	μ	Fit
$1\sigma^2 2\sigma^2 3\sigma^2 4\sigma^2 1\pi^4 5\sigma^2 \underline{2\pi}^2\ ,^3\Sigma$	2.4887	−0.5570459	1.144332	C

(yz) state				(xz) state			
l	$C_{00}^{(l)}$	l	$C_{00}^{(l)}$	l	$C_{01}^{(l)}$	l	$C_{01}^{(l)}$
1	1.320	6	4.391[−2]	0	1.329[−1]	6	1.557[−2]
2	4.477	7	−8.367[−3]	1	−7.806	7	−2.537[−3]
3	−2.119	8	1.365[−3]	2	3.819	8	3.296[−4]
4	7.207[−1]	9	−1.717[−4]	3	−1.320	9	−5.661[−5]
5	−1.960[−1]	10	2.412[−5]	4	3.623[−1]	10	4.242[−5]
				5	−8.164[−2]		

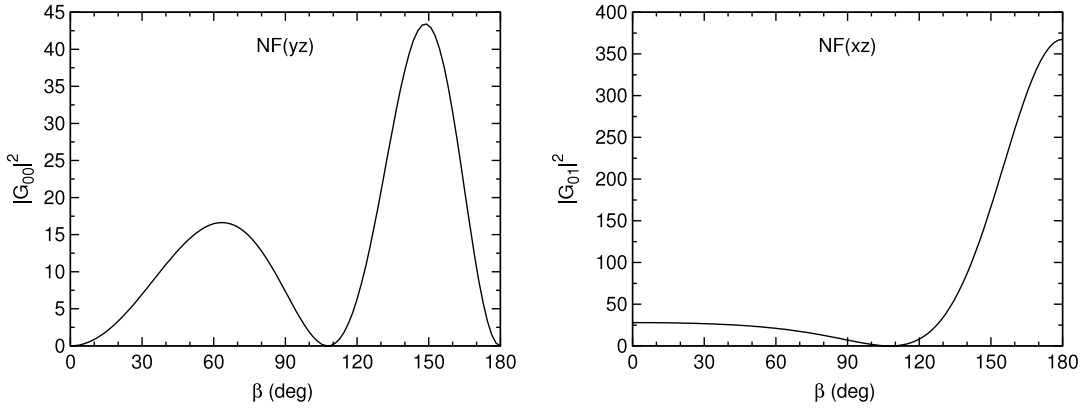

Graph 40. Orientation dependence of the structure factor squared for NF.